EXPLORING THE TECHNICAL & ECONOMIC BENEFITS OF INTEGRATING THERMAL ENERGY STORAGE INTO THE POWER SYSTEM

A Dissertation

Presented to the Faculty of the Graduate School

of Cornell University

in Partial Fulfillment of the Requirements for the Degree of

Doctor of Philosophy

by

Santiago Naranjo Palacio

August 2014

EXPLORING THE TECHNICAL & ECONOMIC BENEFITS OF INTEGRATING THERMAL ENERGY STORAGE INTO THE POWER SYSTEM

Santiago Naranjo Palacio, Ph.D.

Cornell University 2014

In recent years, electricity system operators have recognized the important role that demand-side resources can play in energy and ancillary services markets. As demand-side agents enter these markets, there is growing interest in energy storage technologies to induce flexibility in electric loads. Due to its low cost relative to electrochemical energy storage, thermal energy storage (TES) is a particular focus in the buildings sector. This thesis presents three interrelated projects that explore the economic and technical benefits that TES, when properly operated, can provide to building owners, distribution utilities, and power system operators.

The first project examines the potential of large-scale TES deployment to reduce power system costs in a two-settlement wholesale energy market. I investigate the particular example of shifting cooling loads in the New York State power system on a hot summer day. By solving the system operator's global optimization problem using heuristic methods, I find that TES can reduce both steady-state and transient system costs. TES enables these cost reductions by flattening the system load and reducing generator ramping.

The second project develops a platform that, for the first time in the literature, shows how TES can be used to alleviate power system capacity constraints during critical peak events. This is accomplished by using a set of rate structure packages (RSP) to minimize end-user electricity demand during critical times through optimizing TES operation. Using this platform, I investigate the effect of 42 unique RSP on TES operation and building energy consumption, as

well as the end-user's electricity costs and the utility's costs of operation. Each of these RSP consists of: a seasonal time-of-use electricity rate, a critical peak electricity rate, and a demand response payment level. By simulating building operation under each RSP, I find that there is a set of optimal RSPs that encourage end-user participation without penalizing inflexible loads with excessive critical peak rates.

In the third project, I develop an optimization and simulation platform that, for the first time in the literature, demonstrates the feasibility of using TES to provide spinning reserves. Using this platform, I show that demand-side resources can gain substantial financial benefits by participating in spinning reserve markets, and that capacity payments constitute the majority of these benefits. I then discuss the increase in demand for spinning reserves that power systems will likely see as extreme weather events become more frequent and as more renewable generation is deployed. I conclude by highlighting the important role that demand-side resources can play in meeting future demand for spinning reserves.

BIOGRAPHICAL SKETCH

Santiago Naranjo Palacio was born and grew up in Medellin, Colombia, where he attended Colegio Waldorf Isolda Echavarria. After moving to Gainesville, Florida at age 16, he attended Gainesville High School, from where he graduated in 2003. He enrolled at the University of Florida and earned a Bachelors of Science in Mechanical Engineering with a minor in Material Science in 2008. During his undergraduate studies, Santiago had the opportunity to work in China, Germany, and Thailand, thanks to an NSF, a DAAD, and an IAESTE grant, respectively. After working for a year, Santiago enrolled in the department of Mechanical Engineering at Cornell University in June 2009, where he conducted his graduate research in the Energy and Environment Research lab under the supervision of Dr. Max Zhang. During his graduate studies, Santiago was a visiting researcher at Technische Universität München and RWTH Aachen, where he conducted research on the interaction between building technology and demand-side management programs.

This thesis is dedicated to my friends and family

ACKNOWLEDGMENTS

First and foremost, I would like to thank Dr. Max Zhang, for his support and advice throughout my studies. For being understanding of my unconventional career path and for giving me the opportunity to pursue my goals. For that, I will always be grateful. To my special committee members, Dr. Tim Mount and Dr. Brandon Hencey for their valuable comments. To Dr. Hayley Shen and Dr. Hung Tao Shen, for the continuous support and all of the invaluable career advice. To lab members, Kevin Kircher and Keenan Valentine for sharing their field expertise with me, helping me make my research relevant to a wider audience. To the co-authors in the papers presented in this thesis, listed alphabetically: Sarah Callanan Dr. Brandon Hencey, Kevin Kircher, Keenan Valentine, Myra Wong, and Dr. Max Zhang.

Finally, I would like to thank the Gates Millennium Foundation for their funding support throughout my undergraduate and graduate studies and the Sloan Foundation for their funding support during my graduate studies.

TABLE OF CONTENTS

LIST OF FIGURES

LIST OF TABLES

INTRODUCTION

The effect of human activity on climate change has become quite noticeable, with increasing global temperatures and the incidence of extreme weather events all over the world[1–6]. The U.S. is predicted to be heavily impacted by climate change, where, by mid-century, well over 50% of summer days are predicted to have extreme temperatures[4], with the frequency of heat extremes expected to increase seven-fold by 2040[1]. Moreover, increasing summer temperatures will result in significant increases in electricity consumption[7,8], where increases in maximum daily temperatures will strongly influence peak electricity demand[9].

The effects of climate change are predicted to heighten issues that the power system is currently faced with. For instance, peak power demand growth has outpaced total electricity demand growth in the last decades, resulting in efficiency losses to the electric system, leading to higher electricity prices and electricity system operating costs[10,11]. Furthermore, the power system's aging infrastructure and its constrained capacity, augment system reliability concerns as electricity demand increases[12–14]. All of these issues need to be considered in order to guarantee future operation of the electrical grid.

To maintain system reliability, the electric system operator relies on peak generators, which aside from being costly, emit higher levels of pollution per unit of power output than base load generators[15]. In some areas of the U.S., electricity system operators also make use of demand-side resources in order to maintain a balance between electricity supply and demand, to respond to critical events, and to provide capacity reserve requirements. These demand-side resources respond to price signals sent by the utility provider or system operator by modifying building energy consumption as required by the system. Building operators typically respond to such

signals by allocating their electricity consumption so that financial benefits are maximized without sacrificing building functionality or occupant comfort. Because building cooling systems can account for over 40% of peak demand on a hot summer day[16], they represent a great resource to provide load reduction services during times when the electric system is constrained. To effectively respond to market signals, cooling systems can employ mechanisms to shift or shed cooling load such as thermal energy storage (TES); systems that allow the building operators to incur financial benefits without compromising occupant comfort.

TES represent a group of existing technologies commonly used to shift electricity consumption dedicated to providing cooling load to buildings from periods of high demand and prices to periods of lower demand and prices. This is accomplished by storing thermal load in the form of sensible, latent, or chemical energy, and then extracting said energy to directly provide cooling load to buildings through the heating ventilation and air-conditioning (HVAC) system. Large commercial and industrial buildings often use chilled water systems for cooling, making it economically feasible for said buildings to incorporate thermal energy storage (TES) for demand-side management[17,18],

Previous research on TES has focused on improving the efficiency of the system through advanced control strategies[19–26] and the impact on electricity consumption and prices for individual buildings[27–29], thereby reducing electricity cost to building managers. In this thesis, I am interested in developing practical TES control platforms to assess the technical and financial benefits to end-users, utilities, and system operators, of using TES to provide load management and ancillary services.

In Chapter I, I am interested in quantifying the technical and financial benefits of large-scale TES deployment. To do this, I develop an optimization algorithm to evaluate the benefits to the New York Independent System Operator (NYISO) of optimally allocating a large percentage of the flexible cooling load by using TES. Using this optimization algorithm, I manage to improve the system's load factor, reduce the system's peak to valley ratio, reduce the system's ramping costs, and reduce the total power system operation and capacity costs.

After assessing the benefits that TES could bring to the power system, I conclude that in order to achieve higher TES penetration levels, a wider variety of end-user incentives should exist; benefits that encourage both the proliferation of TES as well as their optimal control. To do this, I explored ways in which the TES could be used in order to provide new types of services to the grid while getting financial remuneration for those services.

Traditionally, TES are used to provide load shifting services in order to reduce system peak load. While such mechanisms work very well to reduce everyday peak load under time-of-use (TOU) rates, there are instances when the power system needs stronger incentives to prevent electricity demand from outgrowing supply. During such events, dynamic electricity pricing and demand-side management programs provide the biggest opportunity to reduce electricity demand. In Chapter II, I investigate the importance of using dynamic pricing in order to encourage electricity demand reduction during critical peak events; times when power system capacity is heavily strained. To do this, I developed a mechanism under which an ice TES operation is optimized to curtail a building's cooling load during critical peak events as a response to rate structure packages (RSP) composed of critical peak pricing and demand-side management curtailment payments. Using this mechanism, TES could be used to provide both load shifting as well as load shedding services; services very valuable to utilities. With this in mind, I set out to

investigate the effect of various RSPs on TES operation and end-user demand profile during critical peak times. Using this information, I determined a set of RSPs that maximize the economic benefits to the end-user and minimize costs to the power system. This set of RSPs show that financial incentives to both end-users and the power system can be increased through the use of innovative TES operation. By enabling TES to respond to critical peak pricing and demand-side management events, the benefits to both end-users and the power system would greatly increase when compared to the traditional TES operation under a TOU rate.

Aside from shifting and shedding energy consumption, there are many reliability services that are crucial to the operation of the power system. In Chapter III, I propose a method through which TES can provide spinning reserves in the ancillary services market and the quantify benefits that an end-user could obtain from doing so. Moreover, this chapter explores the increasing need for a variety of resources to provide spinning reserves in order to counterbalance increasing electricity demand and increasing penetration of intermittent renewable resources.

Finally, I conclude by summarizing all of the major contributions of this thesis.

CHAPTER I

REDUCING POWER SYSTEM COST WITH THERMAL ENERGY STORAGE

Abstract

Thermal energy storage (TES) have been shown to be locally beneficial, helping building managers reduce their electricity bills. Due to increasing interest in TES, it is important for utilities and policy-makers alike to consider the economic implications of increasing TES penetration levels on the electrical system. The aim of this paper is to show that TES can also bring significant benefits to the entire system, and that these benefits are maximized when loads are properly controlled. This paper studies the effect of a heuristic optimal TES load allocation strategy on the New York electrical system's load factor, peak-to-valley ratio, ramping, and operation cost. These results are also compared to different control methods in order to justify the need for such a model and also to justify the results. We first determine the total amount of cooling load that can be shifted in New York State through the use of TES technology by using data from various government agencies. Using a coefficient of performance (COP) model for the chiller to account for efficiency changes throughout the day, the flexible cooling demand for the system is estimated. A method to optimally allocate flexible cooling loads is then used with the goal of reducing the power system cost, while providing the necessary cooling load to keep buildings at comfortable temperature levels throughout the state. Power system cost is determined by using a wholesale energy cost model that was developed using New York Independent System Operator (NYISO) market and load data for both the day-ahead and real-time wholesale markets. By flattening out the system load, increasing the electrical system's load

factor, and reducing system ramping, TES can reduce steady-state and ramping costs, thus reducing the overall power system's operation and capacity costs.

Terminology

COP Coefficient of Performance

DAM Day-ahead Market

L Cooling Load Demand

LMP_{DAM} Locational Marginal Price on the DAM

LMP_{RTM} Locational Marginal Price on the RTM

P_{ave} Average electrical system load

P_{DAM} Electrical Load on the DAM

ΔP_{DAM} Load differential from time to time on the DAM

P_{Fixed} Fixed Electrical Load

P_{Flex} Flexible Electrical Load

P_{Max} Maximum Electrical System Load

P_{Net} Net Electrical Load

P_{RTM} Electrical Load on the RTM

ΔP_{RTM} Load differential from time to time on the RTM

Q Charge/Discharge

Q^{Max} Maximum rate at which storage can charge/discharge

RTM Real-time Market

SOC State-of-Charge

SOC^{Max} Maximum capacity for storage

TES Thermal Energy Storage Load

TES^{Max} Maximum thermal load allowed at one time-step

1. Introduction

In previous decades utilities have seen a shift in electricity demand patterns where peak power demand growth has outpaced the overall electricity demand growth, leading to lower load factors[30], making it increasingly challenging for utilities to plan for both the short and long term. This shift in consumption pattern translates into a less efficient electric system, increasing electricity prices and the overall cost of operating the electric system[10,11]. Moreover, increasing power demand is also a problem because of the current power system's aging infrastructure and constrained capacity[12–14]. Furthermore, because of the increased constraint that these shifts place on the grid, brownouts, blackouts, and other power system strain are expected to occur much more often. These power system reliability issues have an enormous impact on our economy, as blackouts account for over $80 billion in losses each year[31]. In order to increase system reliability, the system currently uses peak generators, which are not only costly, but also emit higher levels of pollution per unit of power output than base load generators[15].

Furthermore, electricity consumption varies significantly from hour to hour, forcing generators to be ramped up or down in order to meet the current demand level. Cycling such generators incurs additional cost due to a decrease in useful life, leading to additional operating and maintenance costs[32,33].

Most electricity is consumed in built environments[34], where building cooling systems can account for over 40% of peak demand on a hot summer day[16]. Large commercial and industrial buildings often use chilled water systems for cooling. In such buildings, it is economically feasible to incorporate thermal energy storage (TES) for demand-side management[17,18], allowing chillers to either generate chilled water/ice to store in an insulated tank, or bypass the tank and directly provide cooling through the building's heating ventilation and air-conditioning (HVAC)

system. Control mechanisms are then implemented to store energy during off-peak hours, when electricity prices and demand are low, and use the energy stored in the tank to provide cooling and reduce electricity consumption during peak times[19,20]. The research on TES has so far focused on improving the efficiency of the system through control strategies[19–26] and the impact on electricity consumption and prices for individual buildings[27–29], thereby reducing electricity cost to building managers. However, little work has been done in analyzing TES in the context of power systems planning and operations, where improved load allocation could significantly reduce the power system costs.

TES can reduce the power system costs through two major mechanisms. First, it can reduce both the steady-state costs (i.e., by shifting load from peak to off-peak periods) and ramping costs (i.e., associated with meeting rapid changing demand or intermittent generation resources) in power system operations. Second, it can also reduce the capacity payments in power systems by decreasing the amount of installed generation capacity needed to maintain system reliability in the long term. This study examines the potential benefits of the large-scale deployment of TES to reduce power system capacity and operation costs (i.e., the steady-state and ramping cost described above) in a two-settlement wholesale energy market and investigates a heuristically optimal load allocation method for shifting HVAC cooling loads in the New York Independent System Operator (NYISO) power system on a hot summer day. In order to have a reference to compare these results to, two other control methods are studied and discussed.

Several assumptions are made throughout this project:

First, most TES technology has focused on large-scale commercial and industrial buildings. To make this study applicable to the current and short-term trends in the U.S., this study concentrates on cooling loads in these two types of building.

Second, in order to evaluate the maximum economic benefits of TES, we assume that the operations of TES in the entire New York State (NYS) can be effectively and centrally coordinated via the NYISO wholesale markets. In reality, TES load coordination will likely require energy aggregators. Developing economic and operating mechanisms among system operators, aggregators and building managers is beyond the scope of this study. In addition, this study does not consider capital, operation, and maintenance costs for TES because these costs are expected to be assumed by end-users and not by the power system operator. This then simplifies the problem to determining the value of reducing operation costs to the power system by coordinating TES operations in the region. The results can be potentially used to design incentives to reduce the costs for installing and operating thermal storages at individual buildings.

Finally, this project seeks to highlight the maximum potential benefits to the system described here by using a particularly hot day. Savings incurred through load shifting will then be reduced for times with fewer cooling load needs.

This paper is organized as follows. First, we determine the amount of cooling load that can be shifted in the NYS region through the implementation of TES, referred to as flexible cooling load (Section 2). Next, we present a method for optimally allocating the flexible cooling load (Section 3). Finally, we compare the results from several allocation scenarios and discuss their implications.

2. Flexible Cooling Power and Load

2.1 Cooling Power and Cooling Load

Describing the operations of TES requires two different frameworks: the power system and the thermal system. The power system deals with electrical power, measured in kW_e, and the thermal system deals with thermal loads, measured in kW_t. To switch from one framework to the other, the coefficient of performance (COP) of the chiller equipment must be used.

For clarity, from here onwards the term Cooling Power will be used when in reference to the power system and the term Cooling Load will be used when in reference to the thermal system.

2.2 Flexible Cooling Demand

This section describes the methods used to determine flexible cooling demand in NYS. In this study, flexible cooling demand is defined as the loads that can be shifted from one time period to another without sacrificing the comfort of the building occupants, which can be expressed as both Cooling Power and Cooling Load.

This study is particularly concerned with summer months, where cooling loads make the largest percentage of total electrical load, overall electric loads have the highest peaks, and system load factors, defined as the average load divided by the maximum load, are the lowest. In order to assess the maximum benefits of TES to the power system, a particularly hot summer is needed; summer of 2006 was one of hottest summers in recent US history. We therefore study June 19th 2006, a sufficiently hot day. The benefits of PEV charging for this day have already been studied[35], making the results from this study more relevant to the on-going discussion on how system loads should be allocated in order to reduce power system cost.

This study deals exclusively with the cooling loads of large commercial and industrial buildings in NYS, as previously discussed. To estimate the flexible cooling load for the NY region, the following data are required: (1) total energy consumption by each sector; and (2) an inventory of buildings for the region, where information is broken down by building type; third, end-use energy consumption for the different sectors; and fourth, an aggregated COP estimate for the entire system.

Sections 2.2.1 and 2.2.2 describe the collection of these data.

2.2.1 Cooling Power Demand

The data needed to estimate the electricity consumption by building type for NYS come from a number of sources. Electricity consumption by sector comes from NYSERDA[36]. The number and types of buildings for the different sectors in NYS are available in the US Census and from the Energy Information Administration (EIA)[37,38]. End-use electricity consumption by building type for the commercial and industrial sectors come from the Commercial Buildings Energy Consumption Survey (CBECS)[39,40] and Manufacturing Energy Consumption Survey (MECS)[41], respectively. This information, in conjunction with prototypical building models developed by Stocki et al.[40], provide an estimate of the end-use electricity usage from the different sectors.

It is important to note that some parts of the cooling system consume electricity on demand, such as pumps and fans, and for the purposes of this study they are considered to be part of the fixed cooling demand. The amount of Cooling Power that is consumed by pumps and fans is estimated by Bekker and Carew[42].

By using estimates for the number of buildings in each sector and the amount of electricity they consume, we construct a bottoms-up estimate of end-use power consumption for each. This

estimate can then be used to separate the total system load, total power, into two categories as seen in Figure 1.1a: flexible cooling power (in kW_e) and fixed power. The flexible cooling power represents the total power as seen by the system that can be shifted to other times through the use of TES. Fixed power represents power demand that cannot be shifted using TES.

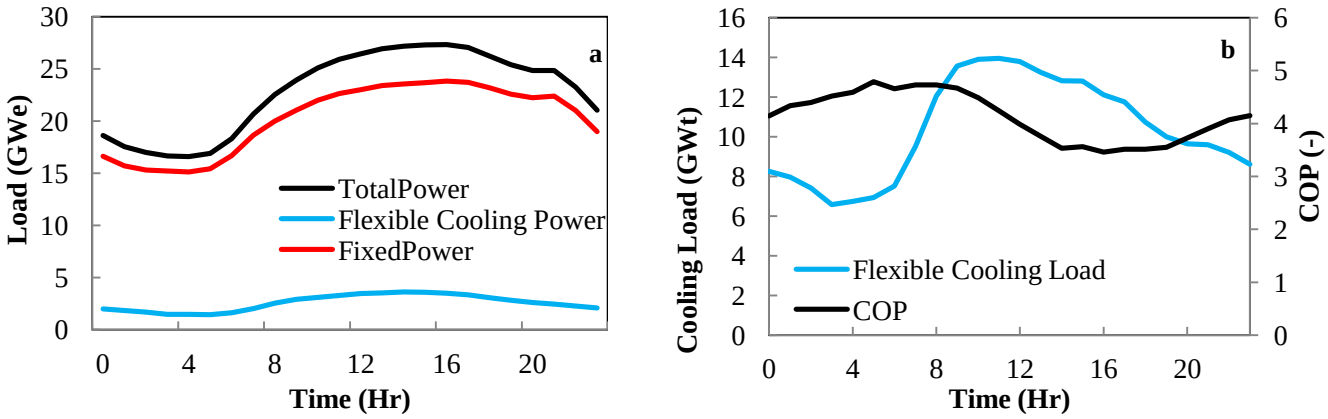

Figure 1.1 (a) Flexible cooling power and (b) flexible cooling load & aggregate COP

As shown in Figure 1.1a, the flexible cooling power demand for NYS accounts for between 8% and 13% of the total power demand throughout the day. The higher percentages take place during mid-afternoon where outside temperatures are high and building occupancy is at its peak, while the lower percentages occur during the early hours of the morning, when buildings tend to be unoccupied and outside temperature are significantly lower.

2.2.2 Cooling Load Demand

The flexible cooling load demand in the NYISO system can be determined by using the flexible cooling power for large commercial and industrial buildings along with the estimated average efficiency of the cooling equipment for the entire region. This average cooling equipment efficiency is estimated with the use of the prototypical building models developed by Stocki et al. [40] along with efficiency measures provided by CBECS [39] and found to be equivalent to a COP

of 3.6. After obtaining the equivalent COP for the region, the diurnal variation of the COP is estimated using the simulation of a constantly loaded 100 Tons (of refrigeration) chiller with a rated COP of 3.6 in a transient building modeling tool, TRNSYS[43], where ambient temperature is the biggest contributor at determining system efficiency.

Figure 1.1b shows the equivalent flexible cooling load (in kWt) demand for New York State along with the average COP estimate for the region. This figure shows that during early hours of the morning and late hours of the night the system COP is higher due to the lower ambient temperatures experienced at these times. During these times, the system performs more efficiently, as described by the COP formulation from a Carnot cycle as seen in Eq. (1), where Carnot cycle represents a theoretical 'perfect' thermodynamic cycle used here to illustrate the effect of ambient temperature on system performance. In this formulation, the effect of the ambient temperature is represented by the condenser temperature, $T_{condenser}$. Using this equation, we can see that with a constant evaporation temperature, T_{evap}, the COP will increase as the ambient temperature decreases. Higher COP implies that the system requires less electricity for the chilling equipment to chill the cooling fluid. The flexible cooling load presented in Figure 1.1b represents that which can be served by either chiller directly or by TES at every hour. Switching between the two cooling mechanisms provides the opportunity to reduce power system costs and improve the system's load factor.

$$COP = \frac{T_{evap}}{T_{condenser} - T_{evap}} \quad (1)$$

3. Mechanisms to Allocate Flexible Cooling Demand

In order to accomplish the goal at hand, this paper uses a model consisting of two distinct parts. The first part of the model describes how TES is introduced into the NYISO framework. Here,

the model accounts for converting electrical loads into thermal loads as well as describing state-of-charge (SOC) of the TES. The second part of the model estimates power system cost for a given load allocation. An optimization algorithm that combines parts of both models is used in order to find the load allocation that minimizes power system cost while satisfying load allocation rules stipulated by the first part of the model.

3.1 System Operation

NYISO's energy market has two settlements: day-ahead and real-time. The day-ahead market (DAM), commits generators with hourly dispatch schedules and produces locational marginal prices (LMPs) for the next day based on predicted load, network constraints, reserve margins, and other grid requirements. The real-time market (RTM) adjusts the generators' committed power outputs and LMPs, on 5-min intervals, to match supply and demand at the time of operation. The DAM costs and adjustments, made by the RTM, determine the total energy market cost for a particular day[35]. In this study, we use 10-min RTM adjustments in order to reduce computation time.

The model uses a hybrid model- and data-based approach to assess the costs of the NYISO energy market. Historical data and market settlement principles are used to create a base case scenario for daily operation. Cost and price changes on generators due to changes in the system's net load are determined by the model, allowing the user to estimate the impact of non-base case scenarios[44].

3.1.1 Load Allocation

This first part of the model develops the net electric load, P, as described by Eq. (2), where net power, P_{Net} consists of the system's fixed electricity demand, P_{Fixed} and flexible, P_{Flex} cooling

power. The flexible cooling power, P_{Flex}, is used in conjunction with the system COP to determine the amount of flexible thermal load provided by TES at every time step as shown by Eq. (3), which is in turn used together with the amount of cooling load demand, L, in order to determine the amount of load charged/discharged, Q, from storage as shown in Eq. (4). $Q > 0$ represents charging and $Q < 0$ discharging. Moreover, the SOC of the system can then be calculated by adding the SOC of the previous time step with the load charged/discharged from the system as shown in Eq. (5).

$$P_{Net,t} = P_{Fixed,t} + P_{Flex,t} \quad (2)$$

$$TES_t = P_{Flex,t} \times COP_t \quad (3)$$

$$Q_t = TES_t - L_t \quad (4)$$

$$SOC_t = SOC_{t-1} + Q_t \quad (5)$$

3.1.2 Power System Operating Cost

The power system cost is assessed by using a statistical approach developed by Valentine et al.[35], where NYISO historical market and operation data is used. In the model, changes in LMP and power system cost are approximated using TES penetration in NYISO, without explicitly employing the techniques of unit commitment and economic dispatch. This model does not couple TES to specific generators, thus providing direct benefit to the entire power system in NYISO through TES dispatch.

The power system data used for this study comes from the NYISO archive, where historical DAM, RTM, and LMP data can be found.

Because of the two-settlement market approach used in this project, all subsequent DAM and RTM net loads are respectively designated P_{DAM} and P_{RTM}, for clarity purposes.

In order to determine daily market energy cost, DAM cost and RTM cost are added as shown in Eq. (6), where the first summation term represents the DAM cost and the second one represents the adjustment cost in the RTM. Here, DAM cost is calculated as the sum over 24 hourly-increments, while RTM cost is the sum over 144 ten-minute intervals. Moreover, power system cost is calculated to be the product of LMP_{DAM} and net load, P_{DAM}, plus the product of LMP_{RTM} and adjusted net load, $P_{RTM} - P_{DAM}$.

$$SystemCost = \sum_{t=0}^{T_1} LMP_{DAM,t}\left(P_{DAM,t}\left|\Delta P_{DAM,t}\right|\right) \times P_{DAM,t} + \sum_{t=0}^{T_2} LMP_{RTM,t}\left(P_{RTM,t}\left|\Delta P_{RTM,t}\right|\right) \times \left(P_{RTM,t} - P_{DAM,t}\right) \quad (6)$$

where the LMP term is a function of steady-state load P, and modulus of the load difference from $t-1$ to t, $|\Delta P|$, and the constants used for the LMP function were obtained from a least-squares regression of NYISO DAM and RTM LMP and load data for 21 summer days from a previous project[35]. Here, $|\Delta P|$ is used to track system ramp magnitudes, which affect system costs. A more detailed discussion of this model is provided by Valentine et al. in[35].

One of the key features of this model is that it explicitly includes costs incurred by the system due to ramping generators, compared to the traditional steady-state dispatch model. The traditional model is constrained only by the physical generator ramp rates, and does not assign costs to the corresponding level of ramping that a generator faces throughout the day. It is clear,

however, that generators incur higher costs when rapidly changing their set-points to match load changes due to an increase in required maintenance and an increase in fuel consumption[45]. These additional ramping costs are captured in the model.

3.2 Load Allocation and Optimization

TES allows energy aggregators to allocate Cooling Power at different times of the day by shifting loads in order to minimize steady-state and ramping costs for the system in the day-ahead and real-time markets. This is done to reduce peak usage, especially during the summer, and to flatten the overall load in order to reduce load-following costs.

A linked two-stage Simulated Annealing optimization that simulates how the DAM and RTM interact, was used in order to determine total power system cost for the day in question. Simulated Annealing is a metaheuristic optimization tool that has been successfully applied to many problems in power systems[35] .

For the day in question, the DAM optimization problem is described by Eq. (7), where the decision variables are the TES thermal load and the goal of the problem is to minimize system cost using information from the DAM and an hourly estimation of the RTM, which will be referred to as E_{RTM}. The optimization is subject to four different constraints, each of which needs to be satisfied both in the DAM and the E_{RTM}. Eqs. (8) and (9) are of the same form as Eq. (2) and seek to allocate TES load. Eqs. (10) and (11) are used to make sure that TES load allocated to a single time-step does not exceed a maximum amount, TES_{Max}. Eqs. (12) and (13) bound the charging/discharging to a maximum rate, Q_{Max}. Finally, Eqs. (14) and (15) bounds the SOC to the maximum storage capacity, SOC_{Max}.

Before the simulation begins, the fixed power is obtained by subtracting the flexible cooling power from the day-ahead load forecast from NYISO. During the first stage, the DAM solver uses the fixed power and initial flexible cooling power allocation in order to obtain the energy market costs. Once this cost is determined, the model attempts to allocate flexible cooling loads to meet cooling demand using TES and reduce power system operating costs. An expected RTM is used in conjunction with historical LMP values to evaluate the effectiveness of the flexible cooling power allocation obtained by the DAM. It should be noted that the DAM does not necessarily allocate all of the flexible cooling load (Eq. (8)), while the expected RTM allocates all of it (Eq. (9)). By doing this, all of the cooling demand will be met, without forcing the DAM to commit to a specific load allocation.

It must be noted here that the minimization is in terms of Cooling Power, while the constraints are in terms of Cooling Loads.

The DAM stage is represented by

$$\min_{TES_{DAM,t},TES_{ERTM,t}} \{LMP_{DAM}(P_{DAM}, |\Delta P_{DAM}|) \times P_{DAM} + LMP_{ERTM}(P_{ERTM}, |\Delta P_{ERTM}|) \times (P_{ERTM} - P_{DAM})\} \tag{7}$$

s.t

$$TES_{DAM,t} \leq L_t + Q_t \qquad \forall t \in (0,..,T_1) \tag{8}$$

$$TES_{ERTM,t} = L_t + Q_t \qquad \forall t \in (0,..,T_1) \tag{9}$$

$$0 \leq 1hr \times \left(TES_{DAM,t}\right) \leq TES_{DAM}^{Max} \quad \forall t \in (0,..,T_1) \tag{10}$$

$$0 \leq 1hr \times \left(TES_{ERTM,t}\right) \leq TES_{ERTM}^{Max} \; \forall t \in (0,..,T_1) \tag{11}$$

$$\left|Q_{DAM,t}\right| \leq Q_{DAM}^{Max} \qquad \forall t \in (0,..,T_1) \tag{12}$$

$$\left|Q_{ERTM,t}\right| \leq Q_{ERTM}^{Max} \qquad \forall t \in (0,..,T_1) \tag{13}$$

$$0 \leq SOC_{DAM,t} \leq SOC^{Max} \qquad \forall t \in (0,..,T_1) \tag{14}$$

$$0 \leq SOC_{ERTM,t} \leq SOC^{Max} \qquad \forall t \in (0,..,T_1) \tag{15}$$

Once the simulation finishes, the minimum cost found so far determines the DAM allocation. This DAM allocation represents the binding Cooling Power hourly allocation that the DAM and generators have agreed to.

The second stage, RTM, of the problem minimizes power system operating cost in the RTM by solving for the real-time load allocation, given the commitments from the DAM as seen in Eq. (16) and is subject to constraints detailed in Eqs. (17)–(20). The RTM now has to allocate all of the flexible cooling power in 10-min increments, as opposed to 1-h increments. This stage uses the regressed LMP model previously described. In this stage, all of the flexible cooling load must be allocated (Eq. (17)) in order to satisfy building cooling demands. Once the simulation finishes running, the RTM allocation with the lowest cost represents the best allocation of flexible cooling power that was found. It must be noted that because of the complexity of the problem and the heuristic optimization used, the solution can only be guaranteed to be a local optimum.

The RTM stage is represented by

$$\min_{TES_{RTM,t}} \{LMP_{RTM}(P_{RTM}, |\Delta P_{RTM}|) \times (P_{RTM} - P_{DAM})\} \tag{16}$$

s.t

$$TES_{RTM,t} = C_t + Q_t \qquad \forall t \in (0,..,T_2) \tag{17}$$

$$0 \leq \frac{1}{6} hr \times \left(TES_{RTM,t}\right) \leq TES_{RTM}^{Max} \quad \forall t \in (0,..,T_2) \tag{18}$$

$$\left|Q_{RTM,t}\right| \leq Q_{RTM}^{Max} \qquad \forall t \in (0,..,T_2) \tag{19}$$

$$0 \leq SOC_{RTM,t} \leq SOC^{Max} \qquad \forall t \in (0,..,T_2) \tag{20}$$

where T1 and T2 represent the number of time intervals for each of the stages, where T1 = 24 is used for the DAM which works in 1-h intervals and T2 = 144 is used for the RTM.

Once the RTM stage has identified an allocation that reduces the system's operating costs, the best solution is stored and a new two-stage optimization starts and the final cost of this new simulation is compared to the best solution so far. This two-settlement optimization process is repeated for a large number of iterations until the system's operating cost and argument variables converge.

3.3 Other Load Allocation Mechanisms

In order to emphasize the importance of the results obtained using the method described on this project two other load allocation control methods are also explored. These methods are described below.

Table 1.1 summarizes the three different methods analyzed on this project. Here, we outline how each of the methods would be controlled, who would control it, and what the purpose of implementing said method would be.

Table 1.1 Comparison between the different load allocation control methods

Method	Who controls?	Primary benefits	Ancillary benefits	Time frame of interest	Information used
System optimization	Energy aggregators	Minimize system cost	Maximize system performance	Day-ahead & real time	LMP system load
TOU without coordination	Building managers	Minimize local electricity bills	–	Months/Weeks ahead	TOU rate structure
Simple system control	System operator	Minimize system cost	Maximize system performance	Day-ahead	System load

3.3.1 TOU without Coordination

Time-of-use (TOU) electricity rates are currently available throughout NYS for large commercial and industrial buildings in order to encourage shifting electrical loads from peak times to valley times. These rates are set by utilities and change based on the season. In order to allow for operation planning, utilities make these rates known a long time before they go into effect. To take advantage of these rates, building managers can introduce TES and charge the TES during the night and discharge it during the day. The TOU without Coordination scenario represents a base case, where each building manager acts individually to minimize their electricity bill, charging the TES at night and discharging it during the day to take full advantage of TOU rates. In order to simplify this case, we assume that TOU rate schedule is identical throughout the state.

3.3.2 Simple System Control Method

If system operators had the power to manage all the thermal loads, they would most likely decide to flatten out the total power seen by the system. To do this, system operators could implement a simple system control method that allocates flexible cooling load using Eq. (21), where P_{Max}

represents the maximum system load, and R (0.58 here) represents a factor created so that the total amount of cooling load provided during the day does not change due to shifting loads.

$$TES_{Flex,t} = \left(P_{Max} - P_{Net,t}\right) \times R \tag{21}$$

By allocating more load to the times where fixed power is lowest and the least load to times where fixed power is highest, the system can see a great improvement on the peak-to-valley differential that is seen on a normal summer day.

4. Results & Analysis

Because the deployment of TES is currently limited in the US, it is important to analyze how an increased penetration of TES would impact the electric grid. In order to do this, we analyze penetration levels between 5% and 40%, where penetration levels are defined as a fraction of the flexible cooling power previously obtained. Each of these is used to represent a milestone for the evolution of TES implementation in the NYS area. For brevity purposes, some of the penetration levels are not displayed in graphs.

4.1 TOU without Coordination

Figure 1.2 shows the load allocation for the TOU without coordination scenario. Here, we see that building managers only operate their chilling equipment during off-peak times. Because all buildings see the same TOU rate, they would all without any coordination choose the same strategy in order to reduce their electricity bill.

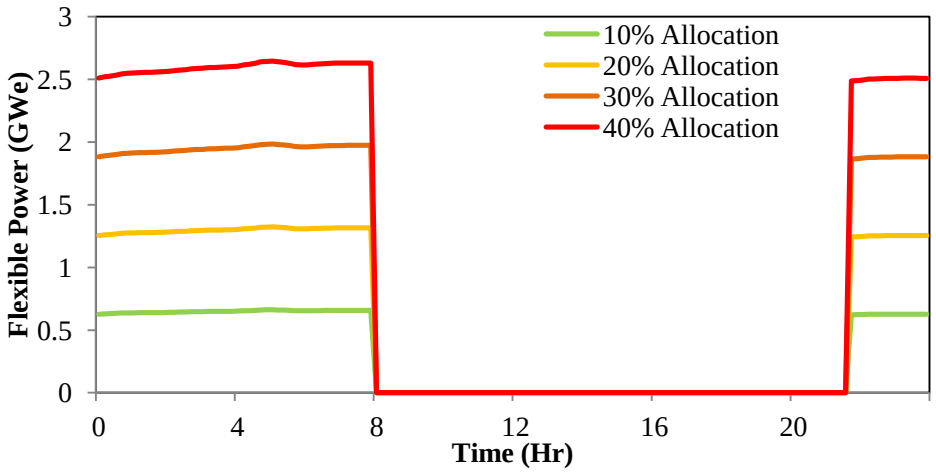

Figure 1.2 Load allocation for *TOU without Coordination*

Figure 1.3 shows the total power that the system sees if the flexible cooling power is allocated using the TOU without coordination method. Here base case represents the original load for the sample day, fixed load represents the load that cannot be shifted and different penetration levels represent the total power after the flexible cooling power has been allocated. In this scenario, all of the building managers charge the TES by taking advantage of TOU rates, leading to considerable ramping for the system during the transition times between high and low electricity rates. Moreover, we see that most of the load is allocated to valley times, with very little loads being allocated to shoulder times, where valley and shoulder represent low and medium load levels.

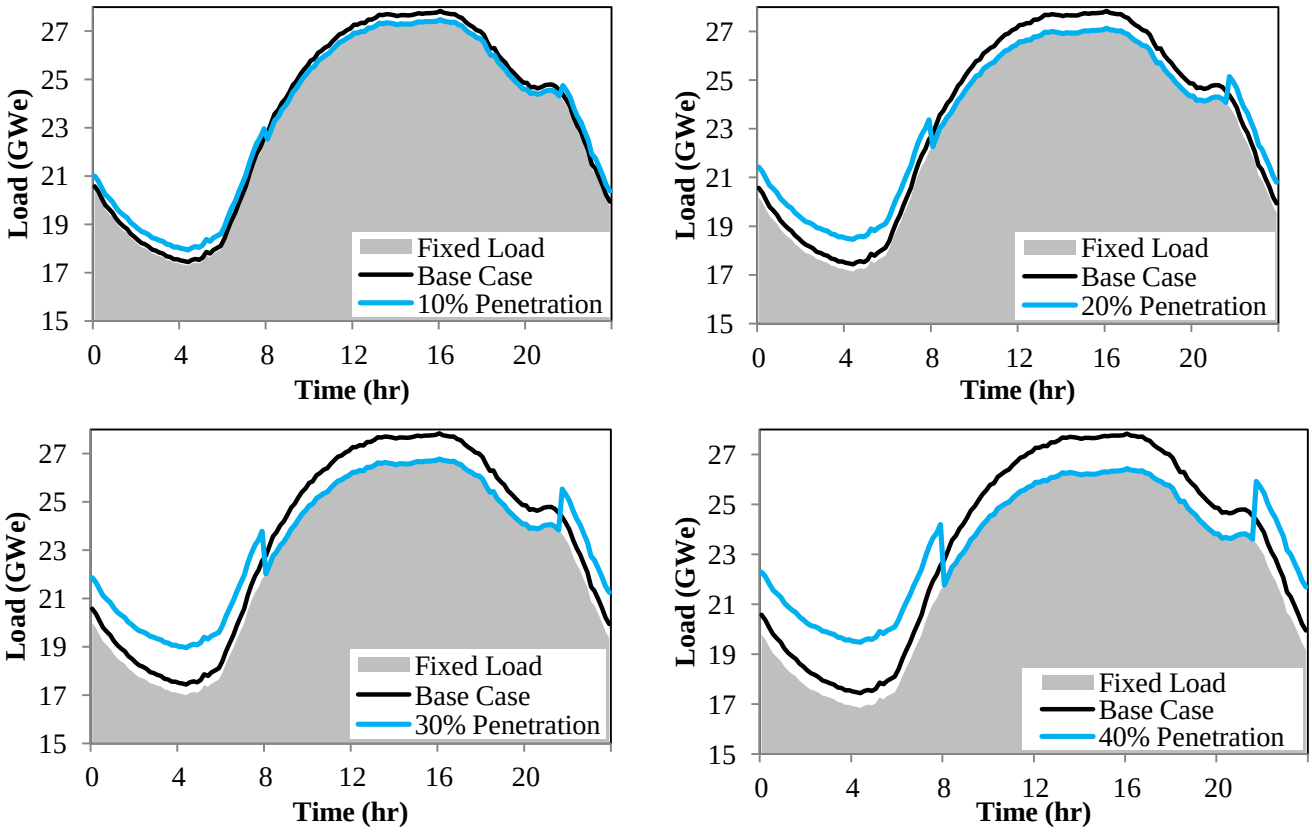

Figure 1.3 Resulting allocations using the *TOU without coordination* control Method

4.2 Simple System Control Method

Figure 1.4 shows how the system operator would allocate loads using the approach previously described. Here we see that most of the flexible load is allocated to early morning and late night, with some being allocated during the late morning and late afternoon hours.

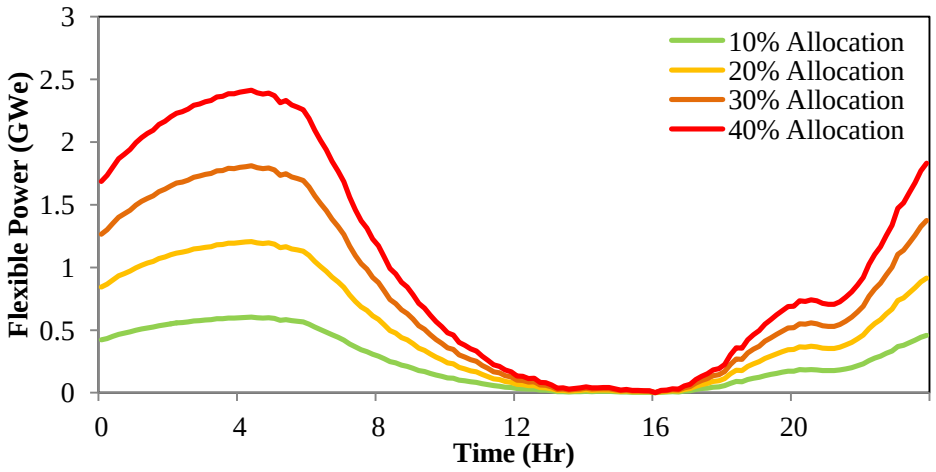

Figure 1.4 Load allocation for *simple system* control method

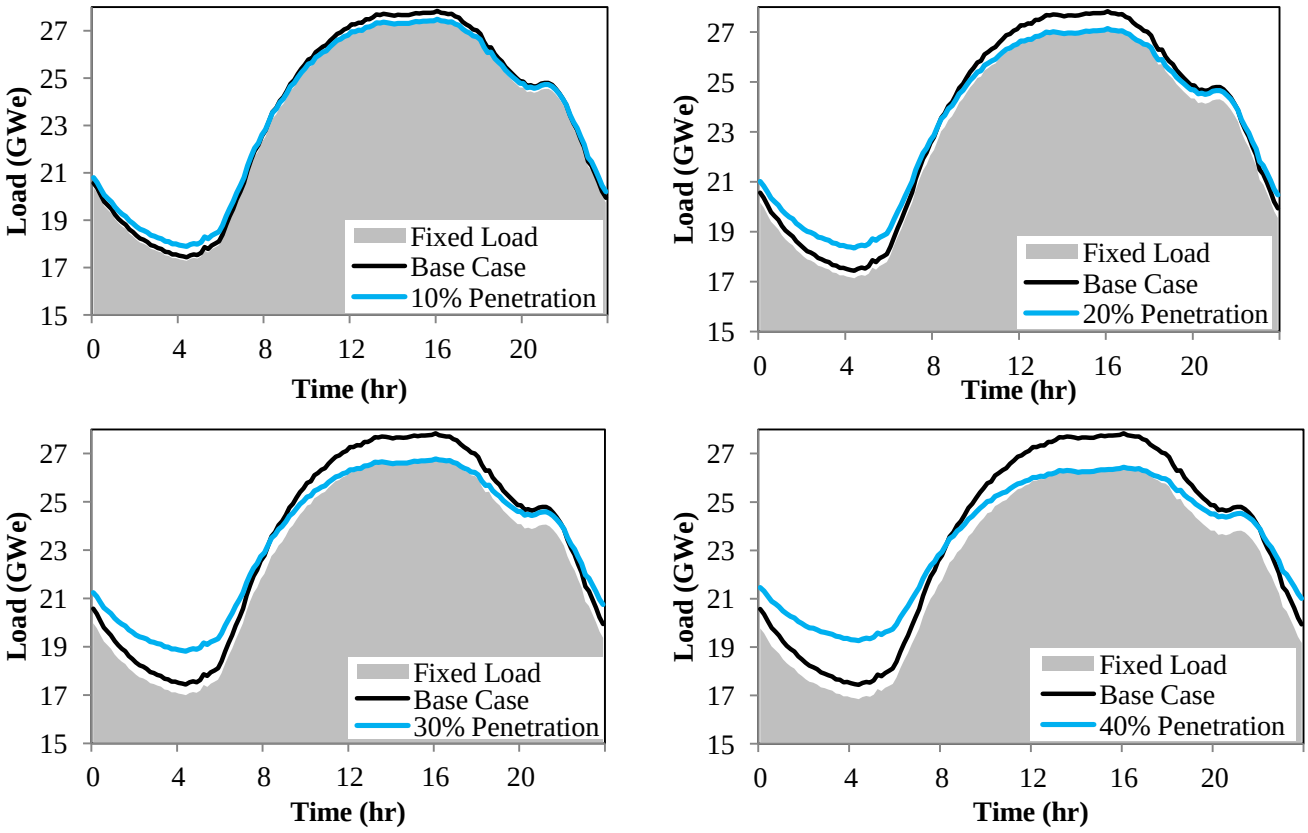

Figure 1.5 Resulting allocations using the *simple system* control method

Figure 1.5 shows the total power that the system sees if the flexible cooling power is allocated using this method. As can be observed here, implementing a simple control mechanism to allocate the flexible cooling load manages to shift cooling power from peak times to both valley and shoulder times. Moreover, using this control method allows the system to shift loads while maintaining a smooth profile, where changes in demand would not greatly disturb system operation.

4.3 System Optimization Method

Before discussing the results obtained using the system optimization method proposed in this paper, it is important to briefly discuss one of the salient features of the method: dynamic system COP. The model described in this paper uses an equivalent system COP in order to take into consideration the efficiency changes due to shifting the time where the cooling equipment is used, because without these considerations, the method would lead to an overestimation of system benefits. In order to demonstrate the usefulness of using a implementing the system COP, we apply the optimization method using a non-varying COP and compare it to the method previously described where COP varies throughout the day.

Figures. 1.6 and 1.7 show the results obtained by using the optimization method with a static and a dynamic COP, respectively. In Figure 1.7 we see that a most of the load is shifted towards valley times, whereas Figure 1.6 shows that the load is shifted to valley times in the early morning and to a lesser degree to shoulder times in the late afternoon. Moreover, Figure 1.6 shows a very similar load allocation pattern for the different penetration levels, whereas Figure 1.7 shows a load allocation pattern that varies as penetration levels increase. These differences can be explained by looking at the COP values from Figure 1.1b, where COP is higher during the early morning times. When COP is taken into account, times with lower COP are not as

favorable because the amount of cooling load that can be produced with the same amount of cooling power is lower than times where COP is higher. Moreover, as penetration levels increase, the balance between ramping cost and COP changes, creating differences on the load shifting patterns. On the other hand, when COP is disregarded, the system allocates load to reduce system ramp and decrease peak usage, creating profiles that vary only slightly between different penetration levels. Both allocations strive to reduce power system operating cost through the reduction of peak load and system ramp, but only one of them makes the necessary considerations for such a system. Having analyzed the system COP, we know that it would not be ideal for the system to allocate loads to times where COP values are low, so we know that the method with COP gives more realistic results.

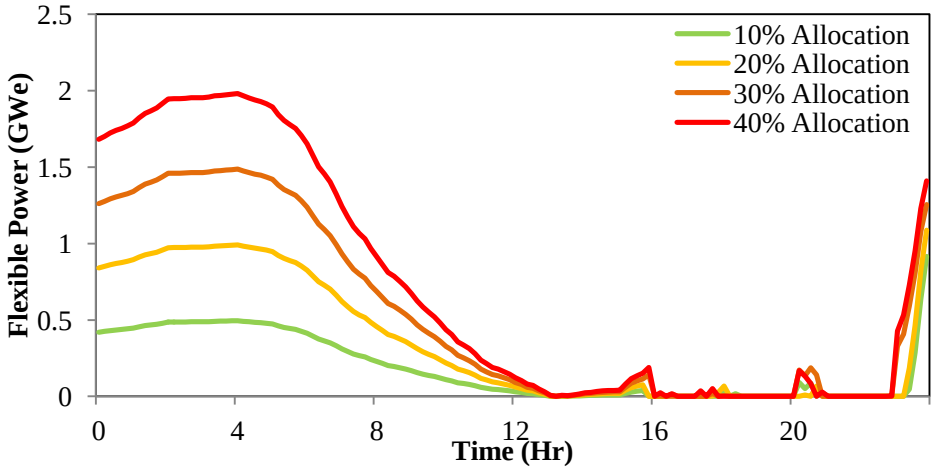

Figure 1.6 Load allocation for *system optimization* control method with static COP

If COP considerations were disregarded from the model, the results would represent an idealized system operation that disregards crucial system parameters, where loads are mostly allocated to both valley and shoulder-times.

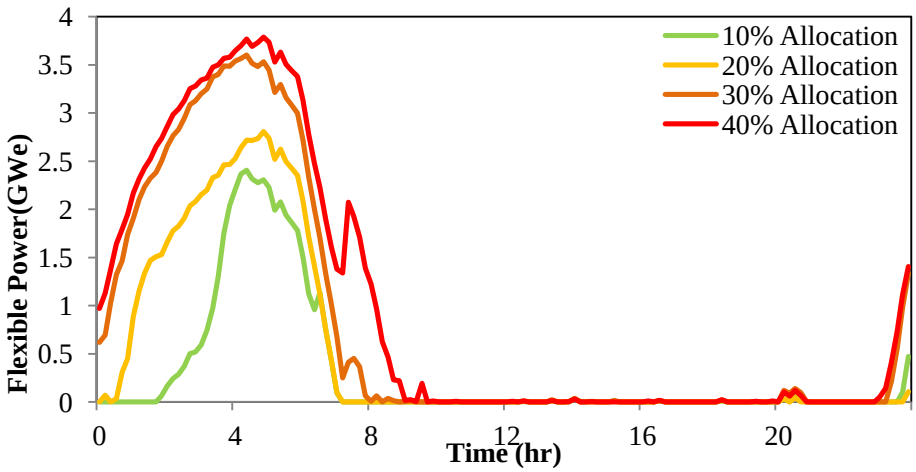

Figure 1.7 Load allocation for *system optimization* control method with dynamic COP

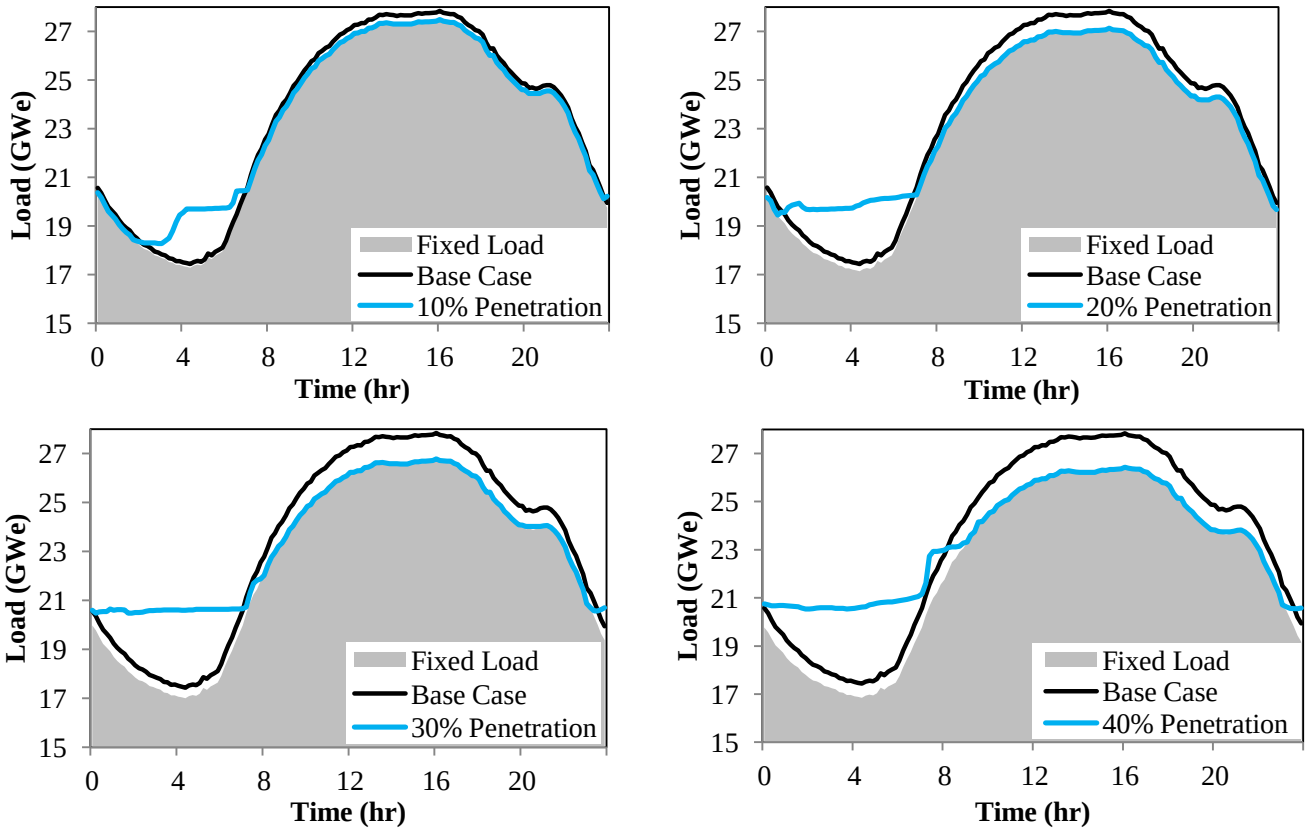

Figure 1.8 Resulting allocations using the *simple optimization* control method

Figure 1.8 shows the total power that the system sees if the flexible cooling power is allocated using the dynamic COP model. Here, we see that this optimization method, aside from shifting loads from peak to valley times, achieves very stable loads throughout the morning for penetration levels of 20% and 30%, thus reducing ramping within the system. For low penetration levels, the optimization method allocates the flexible load to the hours with highest COP values, making the system ramp up significantly twice during the morning hours. For penetration levels of 40%, the valley is completely filled up and loads are also shifted to shoulder times, making the system ramp up significantly once during the morning. For these two cases, we see that system ramp is allowed to increase in order to accommodate load during the most efficient times.

As seen by these results, considering the system COP gives results that are greatly different from those obtained when COP is disregarded, showing that it is important to take efficiency changes into consideration in order to obtain more realistic results. It should be noted here that the results of the optimization method with a static COP will not be further discussed, as they were only introduced with the intent of showing the importance of introducing efficiency measures to the system.

4.4 Metrics

We use four different metrics to measure the performance of the different allocation methods. Those metrics are load factor, peak-to-valley ratio, the ramping incurred by the system, and finally the overall power system cost.

4.4.1 Load Factor

Load factor is defined as the average electrical load, P_{ave}, divided by the maximum load, P_{max}, as shown in Eq. (22), for a given period of time and it is used in the power industry to indicate how efficiently electricity is being used[11]. A small load factor means that the generating capacity is not being used as efficiently as possible, as it shows that only a fraction of all generating capacity is being used at all times. A high load factor then implies that the system is able to make use of most of its generating capacity to deliver power to costumers. Ideally, a system would have a load factor as close to 1 as possible. Figure 1.9 shows the improvement on load factor for one day of operation, using the three methods described here. In this figure, we see that all methods manage to improve the system's load factor, as all of them are shifting loads from peak times to valley and shoulder times.

$$Load\ Factor = \frac{P_{ave}}{P_{Max}} \tag{22}$$

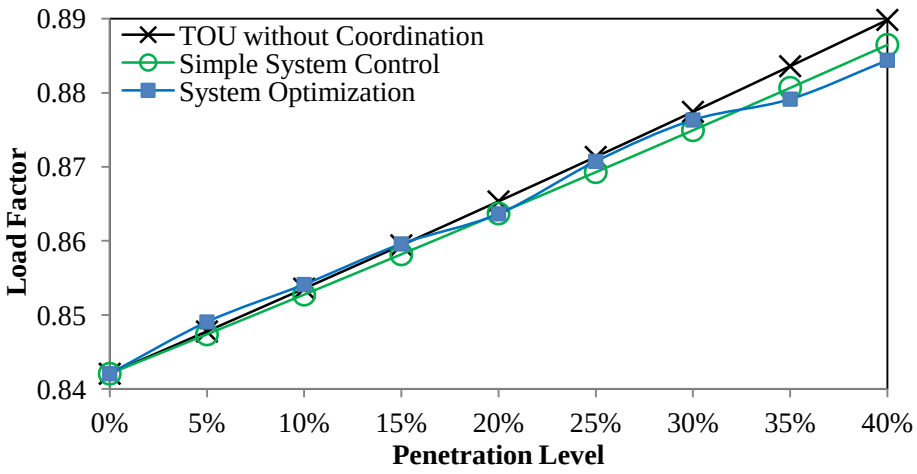

Figure 1.9 Improvements on load factor as a result of increasing TES penetration

All of the methods have similar results because the amount of load allowed to be shifted is the same, meaning that the amount of peak load reduction is very similar for all of the methods and

the small differences between the load factor between the different methods stem from variations on time slots that load is allocated to and the resulting changes to average load as penetration levels increase.

4.4.2 Peak-Valley Ratio

Peak-valley ratio is used to understand how much more generation is needed during the peak times of the day compared to the valley times, and is used as an indicator of steady-state cost associated with power generation. To account for this difference in demand, generators need to be brought online rapidly. These types of generators are often referred to as load-following and peaking generators, and they are usually costly. A high peak-valley ratio means that the system sees peak loads comparably higher than the valley loads, which means the system needs to have a lot of idle generators. A low peak-valley ratio represents a system where the difference in generation from peak to valley is low, which means that a fewer generators will remain idle. For a system operator, it is favorable to have a low peak-valley ratio because it reduces the need for fast ramping generators. Figure 1.10 shows the improvement of peak-valley ratio for the different methods described. In this figure, it can be seen that the optimization method results in lower peak-valley ratio than the other two methods. By shifting a great majority of the flexible load to valley times, the optimization method manages to increase its valley load the most, thus greatly improving the peak-valley ratio.

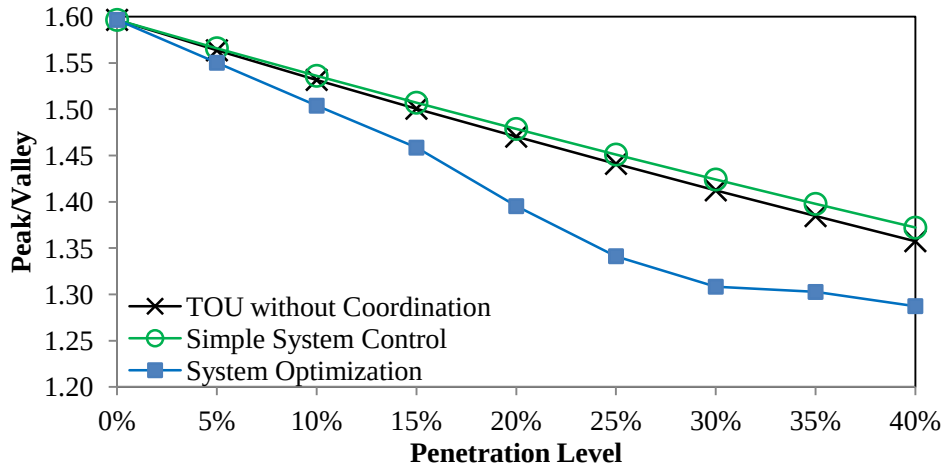

Figure 1.10 Improvements on peak to valley ratio as a result of increasing TES penetration

4.4.3 Ramping

Ramping is used in the electric grid to determine by how much generators have to increase or decrease their electricity production in a short amount of time. Generators operate most efficiently when running at stable conditions, so ramping generators up or down decreases system efficiency. Here, total system ramp, RT, is calculated using Eq. (23), where *i* represents the first hour of the day and T_2 represents the last hour of the day.

$$R_T = \sum_i^{T_2} |P_i - P_{i-1}| \tag{23}$$

Figure 1.11 shows how system ramping changes as penetration levels of TES increase. Here we see that ramping increases significantly for the TOU without coordination case. The reason for this is that given the TOU rate, all building managers will start and stop operating their chilling equipment at around the same times, thus creating two instances during the day where many generators would be forced to be ramped up and down significantly. The other two control methods manage to reduce system ramp, by flattening out the system load.

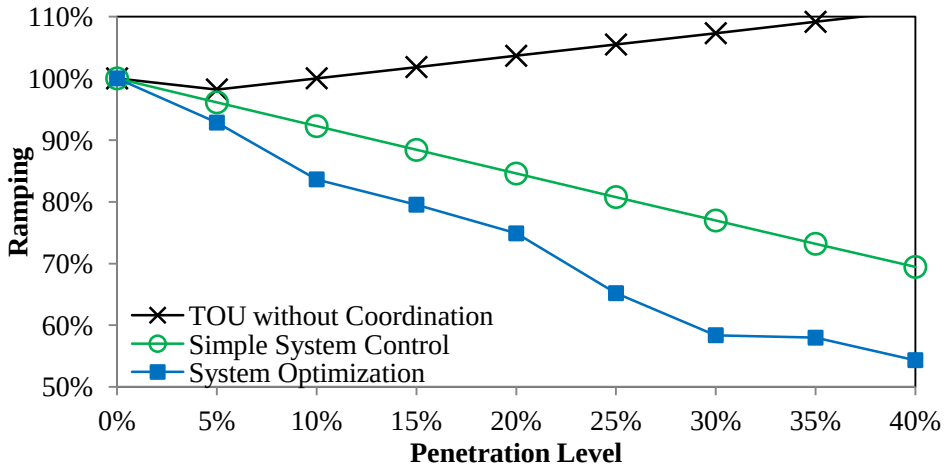

Figure 1.11 Changes in ramping as a result of increasing TES penetration

4.4.4 Power System Operation Cost

Furthermore, if we consider the previous figures, we know that the TOU without coordination method increases system ramping while reducing the load factor and shifting loads from high-price to low-price times. Overall this method manages to modestly reduce system operation cost, as described by Eq. (6), for every penetration level, reducing system operation cost by 0.9% for every 10% penetration level increase. Next, we have the simple system control method that performed better on all previous metrics. This method reduces system operation cost by 1.2% by every 10% penetration level increase. The system optimization method leads to significant ramping and peak-valley reduction. As a result, the system would achieve the best overall cost reduction. This method achieves a 1.5% reduction in system operation cost per every 10% penetration level increase. These results can be seen in Figure 1.12, which shows the percent reduction in cost of operation of the electrical grid for one day, not taking into account the costs of installing or operating TES. For reference, the NYISO cost of operation for July 2006 was $10,269,719[46]. When analyzing this figure, it is important to note that the small reduction in

system cost presented here would translate into hundreds of millions of dollars worth of savings in operation.

For all of the previous graphs, we observed that the TOU without coordination and simple system control methods would produce results that followed a linear relationship, while the system optimization results followed a non-linear relationship. The reason for this, is that due to the COP being incorporated into the calculations, as penetration levels increase loads will be allocated to different times changing the amount of cooling power seen by the system. So, as the penetration level increases, the total load allocation does not vary in a linear way, but rather in relationship to the cooling load allocation along with the COP. The other two methods do not take into consideration the system COP, so they vary linearly in relationship to the penetration level.

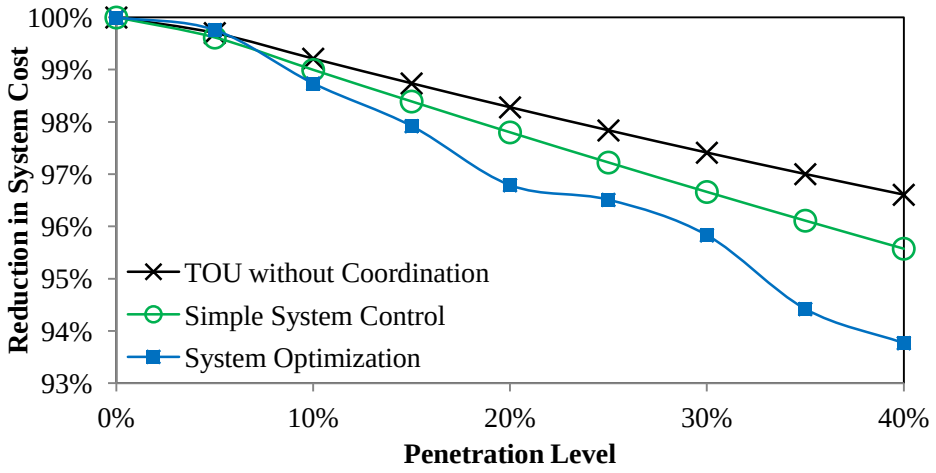

Figure 1.12 Reduction in system operation cost as a result of increasing TES penetration

4.4.5 Power System Capacity Costs

To guarantee system reliability, power systems must maintain an installed reserve margin capacity in order to meet the projected load on the long-term. To accomplish this, resources who

can demonstrate the ability to provide capacity are paid for their services. As a result of increasing peak electricity demand, the payments made to capacity resources are also increasing. By shifting flexible cooling load from peak to valley times, the system's peak load is significantly reduced, reducing the need for increased capacity and their associated costs[47].

Using the simulation data, we seek to estimate the reduction on capacity payments due to an increases penetration level of TES in the New York area. To do this, we estimate the reduction in capacity payments of decreasing peak demand, by using the average capacity price auction for the summer of 2006 ($6.02/kW-Month)[48], and the 18% installed reserve margin requirement for the region[49]. As the peak is reduced through an increase in load shifting, so does the amount of capacity that needs to be available to meet the 18% installed reserve margin requirement, thus reducing capacity payments as seen on Figure 1.13. Here we see that as TES penetration increases, there is a clear reduction of capacity payments (costs).

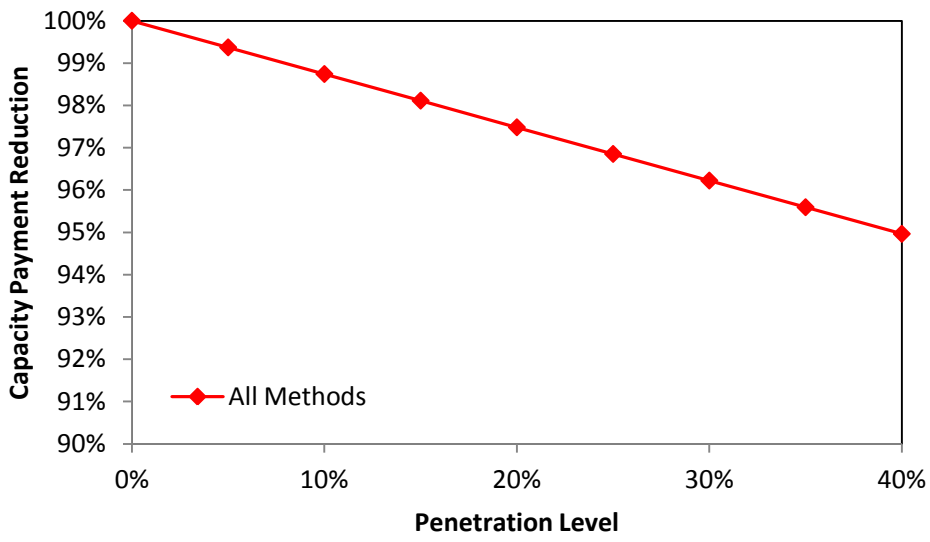

Figure 1.13 Reduction in capacity payments as a result of increasing TES penetration

5. Conclusions

This study investigate how that aggregation and planned allocation of cooling loads through thermal energy storage (TES) can help reduce power system operation costs by reducing peak usage and flattening out the load profile. A system optimization method is used in order to optimally allocate flexible cooling loads and thus improve system performance and reduce power system operation cost. Two benchmark allocation methods, referred to as TOU without coordination and simple system control, are used in order to compare them to the system optimization method. It should be noted that while the two benchmark allocation methods do not achieve as good results as the system optimization method described here, they do manage to achieve significant savings compared to a scenario with no load shifting. Furthermore, dynamic and static COP models were used with the system optimization method, showing how taking these changes into account yields more realistic load allocations.

The results presented here show that all three methods would increase the system load factor by approximately 0.125 for every 10% TES penetration level increase. Moreover, the peak/valley ratio would decrease between 0.56 to 0.77, with the simple system control having the smallest improvement and the system optimization having the highest improvement. Furthermore, ramping within the system would increase by 2.7 by every 10% TES penetration level increase with the TOU without coordination method and decrease by 11.4 by every 10% TES penetration level increase with the system optimization method. Finally, all three methods would achieve power system operation cost reduction in the range of 0.9–1.5% per every 10% TES penetration level increase, where TOU without coordination obtained the smaller reduction and the system optimization method the larger reduction. Finally, through peak load reduction, the power system

can achieve savings on capacity payments of approximately 1.4% for every 10% TES penetration level increase.

Furthermore, TES can provide ramping services to mitigate the variability of generation from renewable sources. Thus, future studies are needed to quantify the benefits of TES in the total power systems costs.

CHAPTER II

HOW THERMAL ENERGY STORAGE CAN ENABLE MUTUALLY BENEFICIAL ELECTRICITY RATE PLANS

Abstract

Thermal energy storage (TES) has been shown to bring significant benefits to end-users and utilities when used in conjunction with time-of-use (TOU) rates. End-users benefit from reduced electricity bills and utilities from decreased loads during peak times. However, TOU rates are modified only a few times a year, and thus are unable to dynamically respond to changes in the system. The benefits of TES can be expanded through more aggressive pricing and demand-side-management programs that incentivize load curtailment during times when the grid is heavily strained. Moreover, the usefulness of current TES optimization methods is limited by the ability of building managers to operate advanced control systems. This paper investigates the effect of using a dynamic critical peak pricing to encourage electricity curtailment during critical peak events. In order to do this, this paper develops a practical platform to optimize building operation and determine a set of rate structures packages (RSP) to reduce financial and operational cost to both end-users and utilities. An array of RSP are developed by overlaying a dynamic critical peak pricing component to an already existing TOU rate and incorporating different curtailment payments during critical peak events. A transient simulation model of a commercial building in New York City is used to find the RSP that reduce the end-user's expenditure on electricity and provide benefits to the utility through an *Optimized Schedule RSP* scenario. A benchmark *Fixed Schedule TOU* is used to create a baseline comparison between the different solutions, and a *Fixed Schedule RSP* is used to demonstrate the importance of optimization. The results outlined in this paper show that there are several rate structure packages that increase global benefits.

Terminology

TES	Thermal Energy Storage
TOU	Time-of Use
RSP	Rate Structure Package
DSM	Demand-Side Management
HVAC	Heating Ventilation and Air-Conditioning
CPP	Critical Peak Pricing
CP	Curtailment Payment
NYC	New York City
COP	Coefficient of Performance

1. Introduction

Historically, market operators have kept electricity prices fixed for most consumers, regardless of actual costs associated with electricity production[50]. This trend is starting to change, with more utilities offering time-of-use rates, critical peak pricing, real-time pricing, or some other type of demand side management (DSM) programs on to its commercial and industrial customers[51]. As a result, energy storage mechanisms have attracted the interest of different players in order to provide load-shifting services during peak times. In the building sector, thermal energy storage (TES) has gained traction as a reliable way for building managers to maintain thermal comfort while reducing electricity payments[52] and providing load-shifting services to utilities[27,52,53].

TES are systems used to shift electricity consumption dedicated to providing cooling load to buildings from periods of high demand and prices to periods of lower demand and prices. Given

diurnal cooling demand and changes in electricity price, TES are commonly used to store thermal load at night and release it later during the day, as needed. This is accomplished by storing thermal load in the form of sensible, latent, or chemical energy, and then extracting said energy to provide cooling load to buildings through the heating ventilation and air-conditioning (HVAC) system.

Thermal storage is a mature technology that has been used for decades to shift commercial buildings' cooling loads away from times of high electricity prices. A typical (cold) thermal storage system consists of one chiller that directly meets load, another chiller that makes ice, and an insulated storage tank. Such systems are typically operated with heuristic schemes like chiller priority, storage priority, or constant proportion control. In recent years, however, various researchers have applied model predictive control to thermal storage, with encouraging results[22,54]. For a precise and readable comparison between model predictive control and these heuristics, see Henze et al.[22]

While model predictive control of thermal storage has shown promise, there are barriers to its uptake in industry. Perhaps most importantly, facilities engineers seldom have experience with model predictive control, and are understandably reluctant to discard working systems in favor of an unfamiliar technology. Another barrier is the fact that many buildings have insufficient automation to enable model predictable control.

In this paper, we propose an optimization-based thermal storage control scheme that is easier to intuit and implement than model predictive control. We restrict attention to three modes of TES operation: (1) ice-making, where the base chiller provides cooling and the ice chiller makes ice; (2) ice-thawing, where cooling is provided from both the base chiller and from melting ice; and

(3) spinning reserves deployment, where the main chiller is turned off and all load is met by melting ice. This reduces the control problem to deciding on the mode of operation at each time step.

We solve the resulting problem approximately using a pattern search algorithm, with the cost function evaluated through building simulation. The simulations are performed in TRNSYS, a commercial software package that solves transient heat flow equations. We argue that this control scheme is both sufficiently simple and -- due to its use of a detailed physical model of the building, rather than the simplified mathematical models employed in model predictive control -- sufficiently grounded in reality to be appealing to working facilities engineers.

Moreover, time-of-use (TOU) rates have been the favored electricity rate when dealing with TES, as constant high night-day electricity price differentials guarantee consistent benefits[55,56] and do not require complex controls. TOU rates, however, are modified only a few times a year[51,57], and thus are unable to dynamically respond to changes in the system. Consequently, TOU pricing alone does not encourage peak reduction during times where the electric system is strained, thus compromising the reliability of the power system, and greatly increasing system costs[58]. To ensure reliable system operation, the power system must then provide enough capacity to meet projected long-term electricity demand, resulting in significant capacity costs to guarantee reliable operation during high peak times.

In order to provide end-users more accurate information regarding the true cost of energy production, a critical peak pricing layer can be added to already existing TOU rates, thus creating a CPP/TOU rate[56]. Under such a rate, customers pay under a standard TOU rate at all times, and, in addition, pay a pre-determined premium, critical-peak-pricing (CPP), for electricity consumed

during critical peak hours. This premium relays the capacity costs the power system incurs onto the end-user and thus encourages peak reduction during critical times. It is important to note, that suitable CPP rates encourage customers to switch loads from critical peak to off-peak times, reducing critical peak loads and benefiting the grid, while very high CPP rates heavily penalize non-flexible loads and will likely deter customers from adopting the CPP/TOU rate structure. The aim of our study is then to develop a framework to identify rate structures that benefit both end-users and utilities. To do this, we analyze the effects of different CPP/TOU rates in conjunction with various curtailment payments (CP) rates on electricity expenditures by the end-users and end-user load distribution during critical peak times. The different CPP/TOU and CP rate combinations will from now on be referred to as rate structure packages (RSP).

To accomplish the goal of our study, we developed a platform on a transient simulation environment, where the operation for the cooling system of a commercial building is optimized for 42 different RSP and compared to the results of having a fixed schedule of operation for the same RSP.

A number of assumptions were made in our investigation, described as follows.

First of all, because the CPP rate serves as a signal to reduce demand during critical-peak hours, demand charges are not considered on this project, leaving energy as the sole measure of electricity pricing.

Second, because consumption peaks during summer months, this paper will only focus on how the system would operate during a hot summer week. A one-week period of the summer 2010 was chosen to represent the maximum benefits that such a system could bring under any of the discussed scenarios. This week provided an interesting study opportunity, in which extreme

temperatures were accompanied by three consecutive critical peak days; highlighting the need for load curtailment during times when cooling demand is highest.

Moreover, because the interest of this paper does not lie on developing a forecast method, real weather and critical-peak hour data is used in order to perform the operation optimizations. Also, operation optimization is only performed for critical peak days as they constitute the highest priority to both utilities and commercial building operators.

Finally, some large commercial buildings receive hourly-differentiated, day-ahead electricity rates, which are not considered here.

This paper is organized as follows. First, we discuss the basic structure of the optimization platform, going into detail on both the physical and financial aspects of the platform. Next, we describe the different scenarios under consideration and describe the different metrics used to quantify cost to end-user and utilities. We then move onto describing the optimization problem and how it was solved. Finally, we move to the results section where we present the results and analysis of these results.

2. Methodology

2.1 Optimization Platform

The system consists of a physical model and a financial model that operate within in a simulation platform, TRNSYS, as shown in Figure 2.1. In order to find the optimal chiller operation given weather, cooling demand, electricity pricing, and critical peak events, an iterative Hooke-Jeeves algorithm, TRNOPT, is implemented within the TRNSYS framework. The physical model

represents the building and the cooling system (HVAC) and the financial model contains information on 42 RSP.

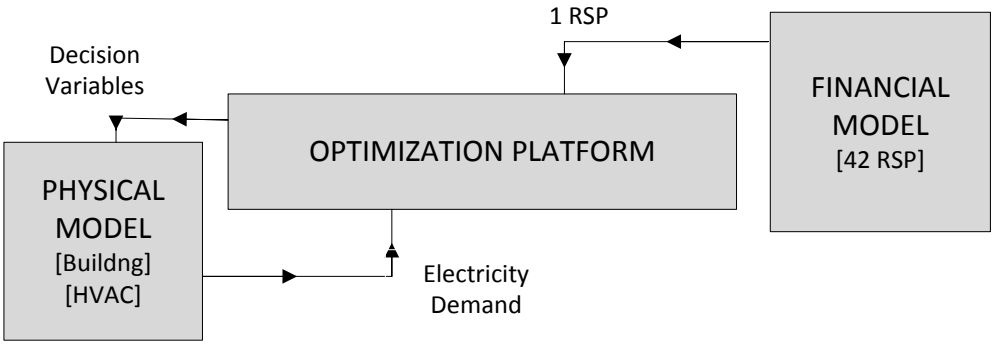

Figure 2.1 Interaction of components with optimization platform, where cost of operation is optimized using information on RSP from the financial model and electricity consumption from the physical model

For a given RSP, a single cycle of the Hooke-Jeeves algorithm includes the following. A vector of 12 decision variables (the on/off times for both chillers for each day under consideration) is sent to the physical model. The physical model then simulates the building's operation under this cooling schedule by solving the partial differential equation system that governs heat flow within the building. The physical model returns the building's hourly power profile to the optimization platform, which compares the cost of that profile to previous iterations and updates the search direction accordingly. The algorithm is guaranteed to converge to at least a locally optimal building schedule; experience suggests that it very often achieves the global optimum.

2.2 Physical Model

The physical model on the optimization platform consists of a building, an ice storage tank, and a two-chiller system. The following sections describe how each of these components was modeled.

2.2.1 Building Model

The modeled building used in this study follows the ASHRAE 90.1 Prototype Building standards[59], which reflects a typical air-conditioned new construction 6-story 306,000 sq-ft office building. A simplified building model for this ASHRAE building is available in the TESS libraries in TRNSYS[60]. This model was modified for this study in order to account for the internal gains of the building and to incorporate an HVAC system in accordance with ASHRAE standards. Schedules for building use and occupancy vary on a diurnal schedule, peaking during normal business hours.

Furthermore, in order to obtain more accurate results, a weather file for NYC for the summer of 2010[61] was developed using actual data as opposed to using a typical metrological year (TMY) file. This method allows us to make a better assessment of how exactly the building and building systems behaved during our study period.

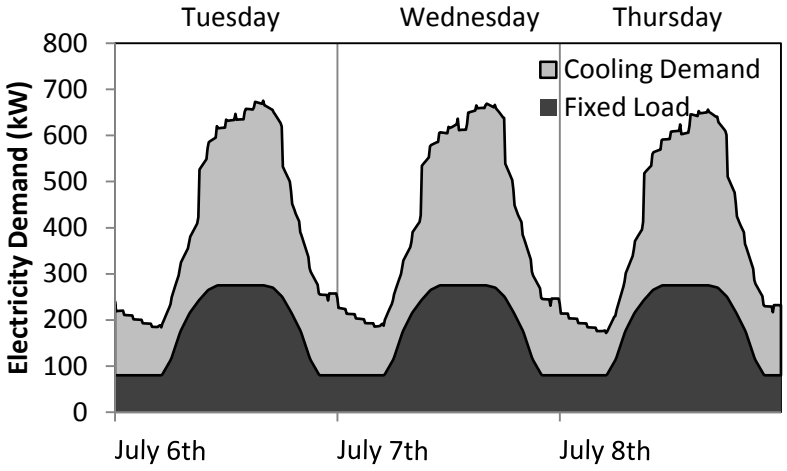

Figure 2.1 Buildings' fixed and cooling load for three critical peak days

This model developed here simulates the cooling load demand the building needs to maintain the thermal comfort in each thermal zone, as specified by ASHRAE standards. Figure 2.2 depicts the variation between day/night cooling demands for this building for three hot days in July 2010.

Total electricity demand for the building is then obtained by estimating the standard *fixed load* electricity consumption profile for lighting, plug-loads, and ventilation systems[62–65], and adding them to the electricity consumption associated with cooling demand. The stacked *fixed load* and *cooling demand* for the building are shown on Figure 2.2, also giving us an idea of what the electricity demand for the building would be if no TES were used.

2.2.2 Cooling System

The cooling system described here consists of a two-chiller system to maintain a good system efficiency and reduce chiller sizing needs[23]. As a result, the system has two separate loops: the glycol mixture loop for ice making and the water loop that provides continuous cooling load to the building. Each of these loops uses pumps in order to provide the desired flow rates for the system. Moreover, fans are used in order to deliver the cooling load from the cooling system to the building.

The system operates in three different modes: ice-making/charging, ice-thawing/discharging, and full curtailment.

The ice-making mode consists of both the glycol and the water loop running independently of each other. The glycol loop is used to transfer cooling load from the *ice chiller* to the ice storage tank, thus making ice, while the water loop is used to provide direct cooling needs to the building. This mode is exclusively used during times when the *base load chiller* can provide all of the cooling needs of the building, which, given cooling demand patterns, happens only during the night and early morning.

The ice-thawing mode goes in operation when the glycol loop is connected to the water loop via a heat exchanger in order to supplement the cooling load. As the heat transfer between the water and glycol loop takes place, the amount of ice available in the storage tank decreases. The discharging mode takes place at times when the *base load chiller* alone does not have the capacity to provide all of the cooling needs of the building. During these times, the *base load chiller* runs at full capacity; providing 30% to 40% of the peak cooling load. This mode is used during late morning to early evenings, when cooling demand is highest.

Full curtailment is a mode of operation that can be used at times where there is a significant incentive to decrease total load, or critical events. This mode functions by turning off the *base load chiller* and providing the entire cooling load through the ice storage tank. A simplified representation of the TES is shown in Figure 2.3.

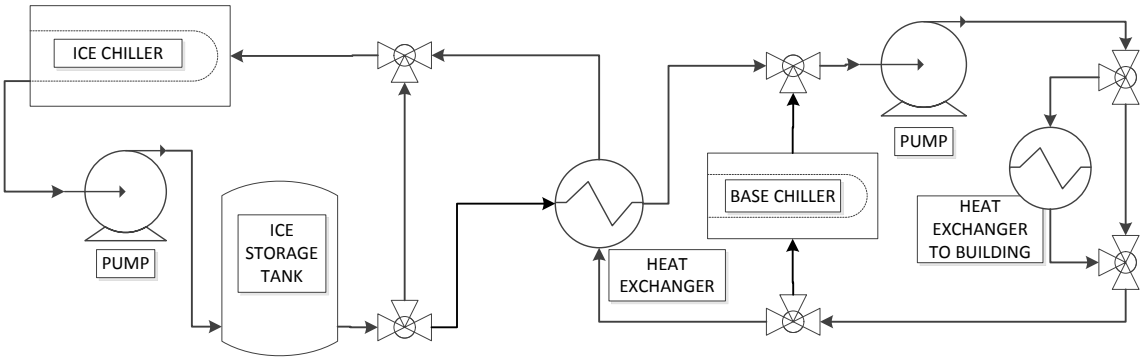

Figure 2.3 Diagram used to represent a two-chiller two-loop system. The two loops operate independently of each other to provide direct cooling to the building and store ice in a storage tank, respectively, and are connected to each other via a heat exchanger when cooling capacity from the storage tank is needed to provide cooling load. The controls used to operate the different valves, are not shown in this diagram

2.2.2.1 Chillers

The cooling system uses two air-source chillers in order to provide the necessary cooling load. The functions of each chiller are divided as such. The *base load chiller* provides all of the cooling requirements at night as well as the base load cooling needs throughout the day. This chiller uses water as a refrigerant and operates at a temperature of 3°C with a rated COP of 3.6. The *ice chiller*, on the other hand, is used exclusively to make ice during the night and remains turned off during the day. This *ice chiller* uses glycol as a refrigerant, operates at a temperature of -6.67°C, and has a rated COP of 2.8. Performance data for both chillers were obtained from chiller data sheets for a TRANE chillers[66].

A simple heuristic optimization was performed in order to estimate what the most suitable chillers sizes would be using the expected operation schedules for each chiller and standards for chiller operation[67]. The result of this optimization suggests that the *base load chiller* and *ice chiller* should have capacities of 180 and 230 tons (of refrigeration), drawing 195 and 287 kW, respectively. These results make sense, that instead of having two-equally sized chillers, the size of the *base load chiller* is reduced and the *ice chiller* increased in order to further take advantage of low electricity prices during off-peak hours.

2.2.2.2 Ice Storage Tank

The ICEPIT ice storage tank developed by Hornberger[68] was used for the TRNSYS implementation of the TES. The parameters for the ICEPIT were obtained following the ICEPIT validation presented by Christophe and Philippe[69]. For our purposes, the ICEPIT was slightly oversized in order to allow for higher cooling storage capability. This configuration provides

cooling through the chiller and the ice storage during normal operation, and uses exclusively the stored ice to provide cooling during CPP events.

2.3 Financial Model

The financial model is used to provide the optimization platform with the different combinations of RSP. This section describes how the CPP/TOU pricing was developed and how CP were incorporated in order to create the RSP.

2.3.1 Developing a CPP/TOU rate

CPP rates are attractive to end-users with load-shifting capabilities because, while imposing high energy costs for ~100 peak hours during the summer, CPP rates offer reduced baseline rates for all other hours during the summer. In this section we describe how this type of rate is created.

In order to create a realistic CPP/TOU rate, we first consider a two-tiered TOU rate with a high/low ratio of 2, as such pricing ratio creates the minimum necessary incentive for TES systems to be implemented based on reductions on energy charges[70]. Then, energy charges for both high and low period had to be determined for this rate. Given that TOU rates for costumers with a demand in excess of 500 kW are typically divided into demand and energy charges, we analyzed TOU rates for small commercial customers[71] in order to have a good reference as to how a TOU rate without demand charges looks like. Using these two guidelines, the TOU rate shown in Figure 2.4 was developed.

Next, to make CPP/TOU rate attractive to consumers, two things have to be considered. First, a desirable high/low TOU pricing ratio should be maintained in order to encourage load shifting during normal operation. Second, the new CPP/TOU rate should be revenue neutral[56]. This

means that a consumer with a flat electricity consumption profile should not see any changes on their electric bill when switching from a TOU to a CPP/TOU electricity rate. To do this, the price of electricity is reduced during non-peak hours. The result of this is that as CPP charges increase, the regular TOU charges decrease for the entire summer. A sample CPP/TOU profile can be seen on Figure 2.4, where a CPP=$1/kWh is used to represent the concept described here. In this project we explore totally 6 different CPP/TOU rates.

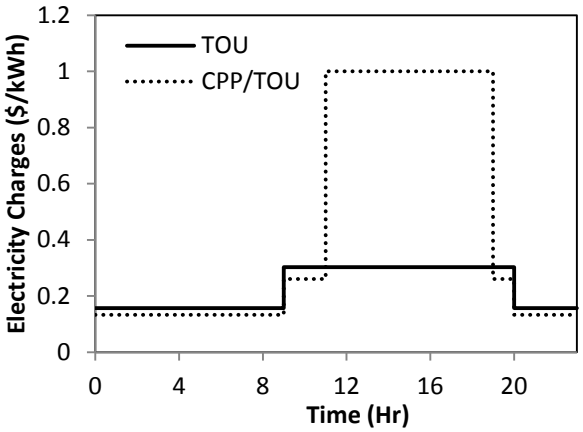

Figure 2.4 TOU and CPP/TOU rates used in this project

2.3.2 Curtailment Payments (CP)

During times of high electricity demand, it is often more cost-effective for utilities to rely on DSM programs to reduce electricity consumption than it is to buy electricity from peak generators. For this reason, most utilities have programs in place, where they pay end-users for curtailment services. For example, utilities offer end-users different incentive systems for load curtailed. We will use two of these programs as reference for our project: Critical Peak Rebate Program (CPRP) and Emergency Demand Response Program (EDRP). Offered by ConEd, CPRP calls end-users to curtail loads during critical situations and pays them $1.5 per kWh of

load curtailed. This program has a minimum reduction requirement of 10kWh/h for costumers with a demand greater than 250 kW and the average participant is called one to two days per year[72]. EDRP, which is offered both by ConEd and NYISO, gives incentives to consumers for load curtailment within a two-hour period of receiving a curtailment notice, by paying costumers the greater of $500/MWh or the locational based marginal price (LBMP) for load reduction. This program requires a minimum reduction of 100 kW by the end-user[72]. EDRP can be used in combination with other demand response programs, as long as only one program is used to pay for the load curtailed[73,74].

As shown by these programs, utilities are willing to compensate end-users for reducing their load consumption during critical peak-time events. We use this information to create 7 CP options that reward customers for any load curtailed during critical peak events, where load curtailed is measured as the increased load reduction when compared to regular operation. Because this project uses a *Fixed Schedule TOU* as a benchmark, we assume that any load curtailed beyond this received CP.

Before discussing rate structure packages, it is important to clarify that the CP is used as a way to offset the high CPP prices that end-users have to pay for their *fixed load*, thus creating an added stimulus for end-users to shift load.

2.3.3 Rate Structure Packages (RSP)

Combining the different CPP/TOU and CP rates, we can create 42 different RSP. For the analysis presented on this paper, both surplus CPP and CP range from $0.0/kWh to $1/kWh with $0.2/kWh increments, with an addition CP of $1.5/kWh to represent the highest payment in the programs considered.

2.4 Critical Peak Hours

Based on electricity demand for the NYC region, the 90 highest load demand hours for summer 2010 were determined. These hours were then defined as the critical peak hours for the summer, as these hours represent the time periods of the year where capacity was likely most constrained. One day could only have one critical peak event, and each event was constrained to a minimum of one hour and a maximum of 12 hours. Next, weather conditions were analyzed for summer 2010 in NYC in order to better understand the relationship between electrical and ambient temperatures.

2.5 Study Period

After analyzing the data for the critical peak hours and weather for the summer 2010, the week of July 4th to July 10th, was identified as of particular interest, as it contained three consecutive critical peak days and had some of the hottest days of the summer. Temperature and critical peak hours for the week are shown in Figure 2.5a) and Figure 2.5b), respectively.

These figures show that Monday, July 5th, while reaching very high ambient temperatures, does not contain any critical peak hours. The reason for this is that this day was the nationally observed holiday after the fourth of July, indicating that a majority of businesses remained closed, resulting in significantly lower electricity demand compared to normal weekday operation. Tuesday, July 6th saw extreme ambient temperatures, generating high electricity demands and creating a 12-hour critical peak event. As the week progresses, ambient temperatures decrease and the number of critical peak hours per day decrease accordingly, allowing the system to reach normal operation by the end of the week. A week like this one challenges the system operator to manage end-loads in order to ensure system reliability while

allowing end-users to continue normal operation. For this reason, we chose this week for our analysis.

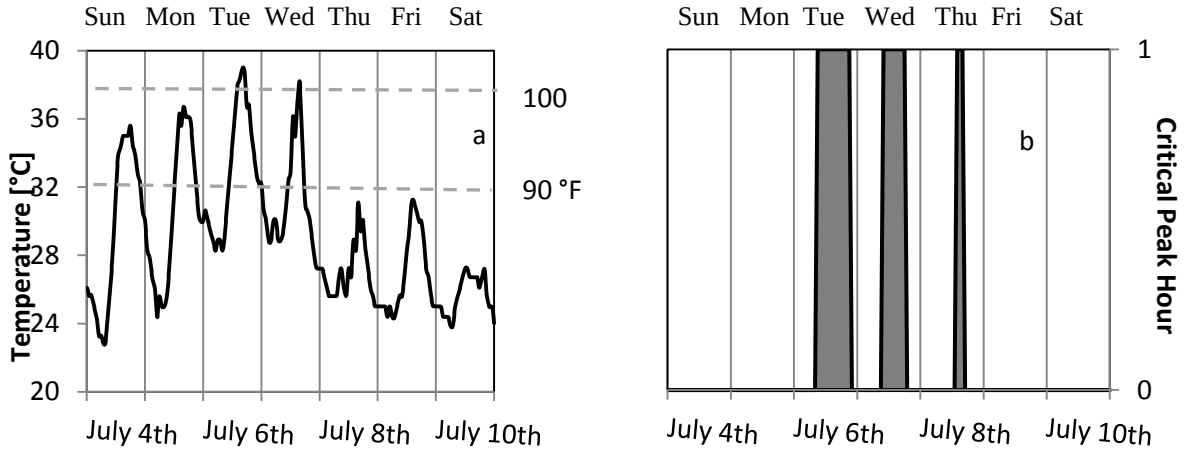

Figure 2.5 Test week a) hourly temperatures b) critical peak hours

2.6 Benchmark Scenarios

In order to be able to use the results from this project, we need to have different methods of operation for the optimization platform. Table 2.1 describes the three different scenarios that are considered on this project and how they are operated.

The first scenario *is called a Fixed Schedule* approach, where the system operates with a pre-determined schedule. Scenario 1.a describes how the system would behave under a TOU rate schedule, where the *ice chiller* operates on a fixed schedule from 12:00 a.m. until 8:00 a.m. in order to produce ice at night and the *base chiller* operates throughout the day. Scenario 1.b then describes how the system would operate once RSP have been introduced. Here both chillers operate on fixed schedules where the *ice chiller* operates from 12:00 a.m. until 8:00 a.m. Additionally, the *base chiller* is turned off from 2:00 p.m. until 8:00 p.m. on critical peak event days.

The next scenario, *Optimized Schedule*, consists of simultaneously optimizing the chillers' schedules with a three-day receding horizon; i.e., Tuesday, Wednesday, and Thursday. This scenario assumes that there is prior knowledge of the demand and retail prices for the entire week. Accurate forecasting for multiple days is not typically reasonable but because that is not the goal of this paper, we assume that 3-day forecasting data is available and accurate.

Table 2.1 Description of the different scenarios considered on this project

No	Scenarios	Rate Structure	Base Chiller	Description
1.a	*Fixed Schedule*	TOU	Remains ON	*TES chiller* runs for 8 hours at night while the *base chiller* runs 24 hours a day
1.b		RSP	Turns OFF	*TES chiller* runs for 8 hours at night while the *base chiller* is turned OFF 6 hours during the day
2	*Optimized Schedule*	RSP	Turns OFF	Operation of *TES & base chiller* is optimized with a 3-day prediction horizon

2.7 Metrics

Monetary metrics are used in order to determine how different scenarios and rate packages benefit the end-user. The benefits the utility receives from load reduction from one single building are, however, rather difficult to measure, as information regarding congestion, generation, and other data that would help determine how much the utility benefits from this reduction is not readily available. For this reason, we rely on operation and monetary metrics in order to characterize how different scenarios and rate packages perform with respect to the interests of the utility.

2.7.1 Electricity Cost (g_e)

Let $P \in \mathbb{R}^{24\times7}$ be a matrix containing the average power consumption P_{ij}(kW) during the i^{th} hour of the j^{th}day for an entire week. Let P^B be defined similarly for the benchmark *Fixed Schedule TOU* scenario. Then the electricity cost ($) is

$$g_e(P) = \sum_{j=1}^{7}\sum_{i=1}^{24} c_{ij}P_{ij}\Delta t$$

where c_{ij} ($/kWh) is the cost of electricity in the i^{th} hour of the j^{th}day, and Δt = 1 hour.

2.7.2 Curtailment Payments (g_c)

The curtailment payments ($) are

$$g_c(P) = \sum_{j=1}^{7}\sum_{i=1}^{24} \kappa_{ij}\left(P_{ij}^B - P_{ij}\right)$$

where κ_{ij}($/kWh) is the curtailment payment rate in the i^{th} hour of the j^{th}day.

2.7.3. Occupant Disutility Cost (g_d)

The building operator also incurs a cost for unmet cooling load, which we call the occupant disutility cost and define as

$$g_d(P) = c_d \sum_{j=1}^{7}\sum_{i=1}^{24}\left|Q_{ij}^{req} - Q_{ij}\right|$$

where Q_{ij}^{req} and Q_{ij} are the required cooling power and the cooling power actually delivered during the i^{th} hour of the j^{th}day, and c_d (\$1/kW) is the cost incurred by the building operator for failing to deliver 1 kW of desired cooling power.

2.7.4 Load Distribution Cost (g_l)

Let $\bar{P} = (P_1, P_3, \dots, P_N)$, where $P_1 \leq P_2 \leq \cdots \leq P_N$, be a sorted list of the building's power consumption during the N critical peak hours, with a $\bar{P}^B$ defined similarly for the *Fixed Schedule TOU* power profile. Let

$$P_{(k)} = \max_{i \in \{1,2,\dots,N\}} P_i$$

$$s.t. \quad \frac{P_i}{P_N} \leq k$$

be the 100kth percentile of $\bar{P}$ (so $P_{(0.2)}$ is the 20th percentile of $\bar{P}$, $P_{(1)} = P_N$ is the maximum element of $\bar{P}$, and so on). Then the load distribution cost of $\bar{P}$ is the following weighted sum:

$$g_l(\bar{P}) = c_l \sum_{\kappa \in \mathrm{K}} \kappa P_{(k)}$$

where

$$\mathrm{K} = \{0.2, 0.4, \dots, 1\}$$

and c_l (\$/kW) is the utility's load distribution cost. Since we don't have direct access to c_l, we leave it as a tunable parameter. The purpose of the load distribution cost is to penalize power profiles with high peaks, even if those peaks occur only rarely.

2.7.5 Ramping Cost (g_r)

The ramping cost ($),

$$g_r(P) = c_r \sum_{j=1}^{7} \sum_{i=1}^{24} \beta_{ij} \left| P_{ij} - P_{(i-1)j} \right|$$

penalizes rapid fluctuations in the building's net load. Here β_{ij} = 1 $/kW during peak hours and zero otherwise, and c_r ($/kW) is the cost incurred by the utility for a one kW ramp over one hour.

2.8 Cost Calculations

Using the above-described metrics, monetary and operation costs to the end-user and the utility are calculated respectively for each different case and rate package.

2.8.1 End-User Cost (J_b)

The net cost of a power profile P to the building operator is

$$J_b(\mathrm{P}) = g_e(P) - g_c(P) + g_d(P)$$

2.8.2 Utility Operation Cost (J_u)

The net cost of a power profile P to the utility is

$$J_U(\mathrm{P}) = g_c(P) + g_t(P) + g_r(P) - g_e(P)$$

2.9 Optimization Method

Once the platform has been set up, an optimization method is needed to negotiate trade-offs between occupant satisfaction and electricity expenditures. We employed a Hooke-Jeeves pattern-search algorithm to optimally schedule the building's cooling system. Pattern-search or direct-search optimization is a heuristic method predominantly used in conjunction with simulations to optimize the operation of a complex physical system. In particular, this method has shown to give good results when dealing with HVAC operation, where it has been used to reduce electrical costs[75] as well as energy consumption[76].

The Hooke-Jeeves method was implemented using the TRNOPT tool in TRNSYS. The objective function is the building's total cost, $J_B(P)$. It includes three terms: the cost of electricity, the cost of occupant dissatisfaction due to unmet cooling load, and the curtailment benefits provided by the utility for load reductions. There are twelve decision variables: the start-up and shut-down times for both the *ice chiller* and the *base load chiller* (four variables per day) for Tuesday, Wednesday and Thursday. The decision variables are subject to feasibility constraints defined by the authors in order to reduce the cardinality of the search space. These constraints are defined heuristically as follows.

Let x_1 be the start-up time of the *ice chiller* on Tuesday (first day where schedule is optimized). The *ice chiller* start-up constraint is $x_1 \in \mathrm{X}_1$, where

$$\mathrm{X}_1 = \{0, 0.5, 1, \ldots, 7.5, 8\}$$

i.e. the *ice chiller* may turn on at any half-hour interval between midnight and 8:00 AM. Let x_2 be the shut-down time of the *ice chiller* on Tuesday. The ice chiller shut-down constraint is $x_2 \in \mathrm{X}_2$, where

$$\mathrm{X}_2 = \{8,8.5,9,\ldots,15.5,16\}$$

i.e. the ice chiller may turn off at any half-hour interval between 8:00 AM and 4:00 PM.

The constraints on the *base load chiller* are defined similarly. Let $x_3 \in \mathrm{X}_3$ and $x_4 \in \mathrm{X}_4$ be the start-up and shut-down times of the main chiller. Then

$$\mathrm{X}_3 = \{10,10.5,11,\ldots,17.5,18\}$$

$$\mathrm{X}_4 = \{16,16.5,17,\ldots,23.5,24\}$$

i.e. the *base load chiller* can turn be turned off between 10:00 AM and 6:00 PM and be turned back on anytime between 4:00 PM and midnight. Here it is important to note that if this chiller is turned on before being turned off results in the chiller remaining on for all times during that day.

For Wednesday, $x_1, \ldots x_8$ (the on- and off-times for each chiller) and constraint sets $\mathrm{X}_1, \ldots \mathrm{X}_8$ are defined similarly, with (for example) X_5 offset from X_1 by 24 hours. For Thursday, the constraint set X_9 is offset from X_1 by 48 hours, and so on. Thus the feasibility constraint can be written as $\in \mathrm{X}$, where $x = (x_1, \ldots, x_{12})^T$ and

$$\mathrm{X} = \{x \in \mathbb{R}^{12} \mid x_i \in \mathrm{X}_i \text{ for all i}\}$$

Summarizing, the building operator's optimization problem is

$$\boxed{\min_{x \in \mathrm{X}} J_b\big(P(x)\big)} \tag{1}$$

where $P(x) \in \mathbb{R}^{24\times7}$ is the power profile resulting from the on/off times in x, determined through TRNSYS simulation. Problem (1) is an integer program with a non-continuous, non-differentiable cost function that requires significant processor time to evaluate. This motivates our use of the Hooke-Jeeves pattern-search algorithm.

3. Results and Analysis

3.1 Results

A graph to describe the optimization at hand, comparing the end-user and utility operation costs is shown as Figure 2.6. This graph displays the trade-off between the different cases and RSP used, where an optimal solution would minimize the cost for both end-user and utility.

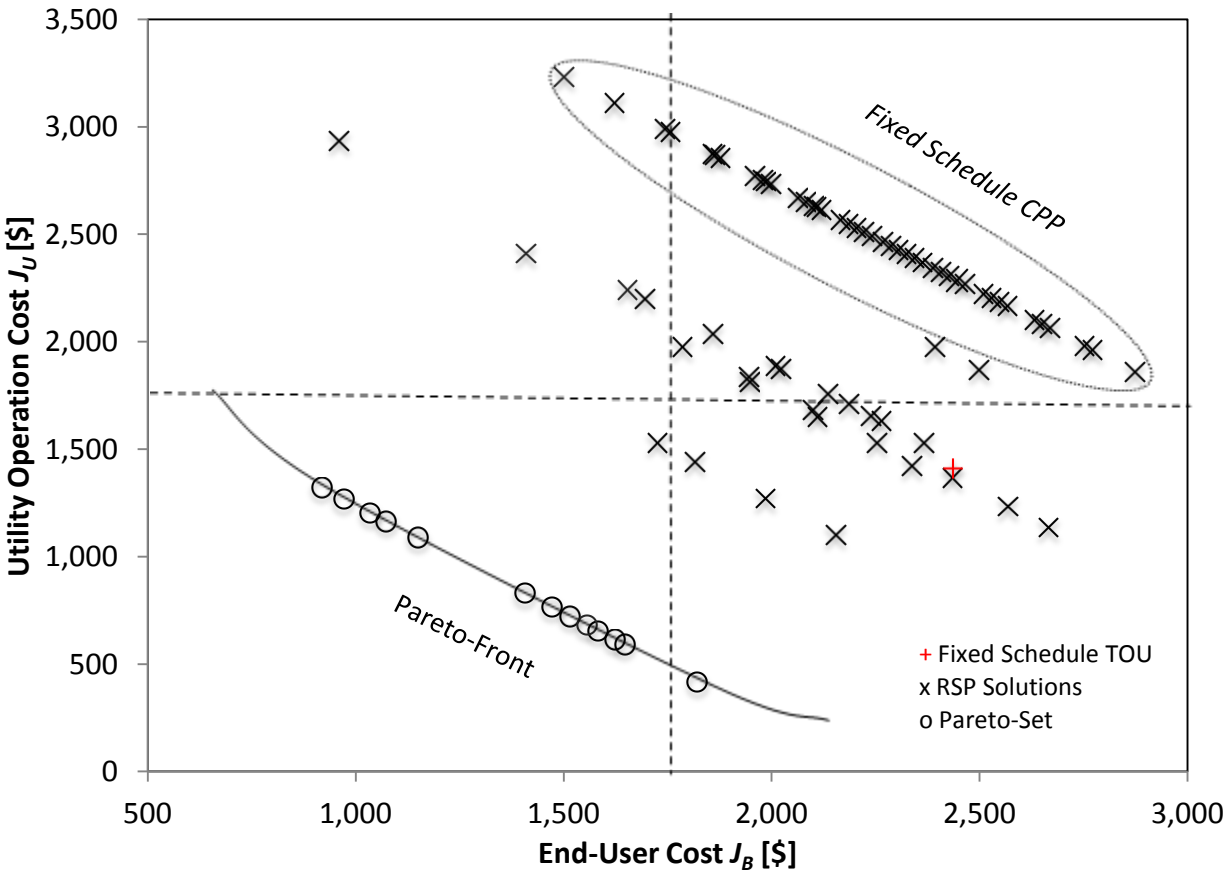

Figure 2.6 Benefit comparison graph between end-user cost and utility operation cost

In Figure 2.6, the red-cross marks the solution achieved by the *Fixed Schedule TOU* and thus defines the benchmark to which all results need to be compared to. This solution is expensive to the end-user, J_B, at ($2436) but provides low cost to the utility, J_u, at ($1410). Next, the *Fixed Schedule RSP* solutions are located on the upper right-hand quadrant of the graph, ranging from median to high cost to the utility, J_u ($1859 to $3231), and to the end-user, J_B ($1500 to $2873). The remaining solutions are part of the *Optimized Schedule RSP* and we see that they provide solutions that range from cheap to costly for both the utility, J_u ($722 to $ 2935), and the end-user, J_B ($960-$2664). It is important to note, that the entire set of *Optimized Schedule RSP* solutions achieve median to low costs in at least one of the metrics measured.

Furthermore, because a trade-off metric between cost to end-user and utility cannot be quantified given the known information, there is a set of 13 solutions whose results need to be considered to be equally good as shown in Figure 2.6. This set of solutions is referred to as the Pareto-set, or non-dominated solutions[77], and the members of the set are presented on Table 2.2. The Pareto-set solutions are used to compare the best case scenario against the *Fixed Schedule TOU* in the following sections.

Table 2.2 End-user and utility cost for pareto-set solutions

RSP [CPP/CP]	End-user Cost [$]	Utility Cost [$]	RSP [CPP/CP]	End-user Cost [$]	Utility Cost [$]
0.4/1.5	917.65	1320.8	*0.2/0.8*	1515.95	722.5
0.2/1.5	970.86	1267.59	*0.8/1*	1555.96	682.49
0.6/1.5	1035.07	1203.38	*0.4/0.8*	1582.12	656.33
0/1	1073.16	1165.29	*1/1*	1623.75	614.7
1/1.5	1149.35	1089.1	*0.6/0.8*	1646.33	592.12
0.4/1	1407.48	830.97	*0.6/0.6*	1820.97	417.48
0.6/1	1471.68	766.77			

3.2 Individual Cost Consideration

In order to better understand how operation and financial cost affect the different solutions on Figure 2.6, we analyze results for each cost factor individually and compare them to the end-user cost.

3.2.1 Operational Consideration

Here, we compare the individual contributions of load distribution cost and ramping cost to the end-user net cost. Here, it is important to note, that the occupant disutility cost is negligible for every solution, so it will not be discussed further.

The benchmark scenario, *Fixed Schedule TOU,* scores very well in ramping cost, g_r ($724), but poorly in load distribution cost, g_l ($3121).

All solutions under the *Fixed Schedule RSP* scenario obtain the same results under load distribution cost, g_l ($2542), and ramping costs, g_r ($2190), as shown on Figure 2.7a) and 2.7c), respectively. We can conclude then that when monetary costs are not considered the *Fixed Schedule RSP* gives a solution comparable to that of the *Fixed Schedule TOU* as the ramping cost, g_r, showed an increase of (202%) and a load distribution, g_l, reduction of (19%). Although the increase in ramping cost is greater than the level reduction cost, we do not have a metric to compare the value of these two parameters, so we cannot conclude which of the solutions is better.

Finally, *Optimized Schedule RSP* scenario creates solutions with varying operation utility costs. Figure 2.7b) and 2.7d) show us the ranges of solutions obtained for load distribution cost, g_l ($1617 to $2210), and ramping cost, g_r ($621 to $2162), where the solutions marked with 'o'

represent the Pareto-set solutions. As shown in these graphs, when compared to the benchmark scenario all of the solutions decrease load distribution cost, g_l, by (30% to 48%). In terms of ramping cost, g_r, however, some solutions decrease the cost (14%) while others increase it (56% to 198%). So, for the entire scenario, we cannot conclude which solution is better. However, we see that all Pareto-set solutions decrease load distribution and ramping costs when compared to the benchmark, so we can conclude that this set of solution yields to better operation cost to the utility.

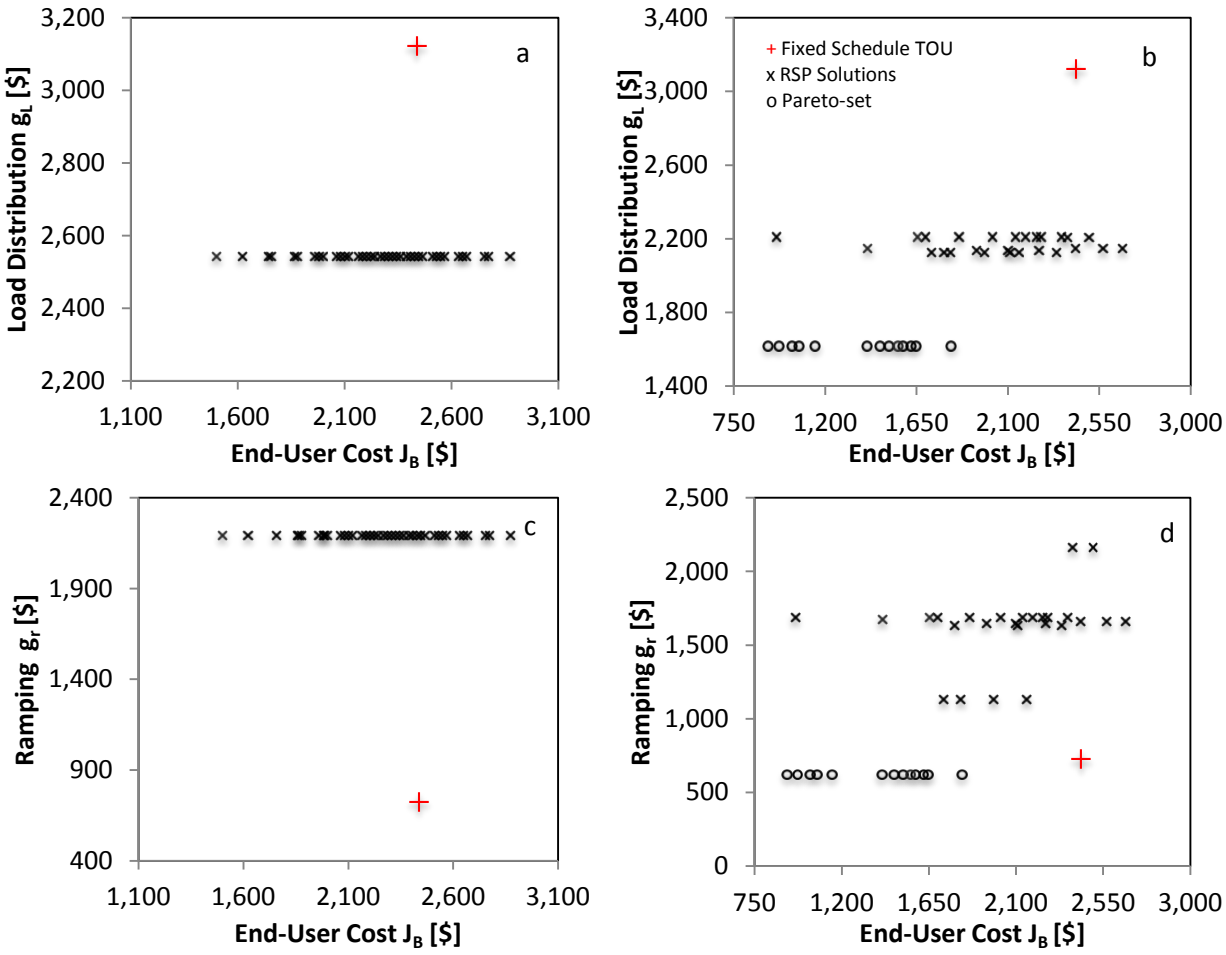

Figure 2.7 Benefit comparison for different solutions between:
a) J_B vs. g_L for *Fixed Schedule CPP* b) J_B vs. g_L for *Optimized Schedule*
c) J_B vs. g_r for *Fixed Schedule CPP* d) J_B vs. g_r for *Optimized Schedule*

3.2.2 Financial Considerations

Now we want to analyze the results in terms of financial costs. To do that, we compare the cost of electricity to the curtailment payments, as well as the net cost to the end-user and the curtailment payments made by the utility. We do this in order to understand how cost of electricity and curtailment payments relate to each other.

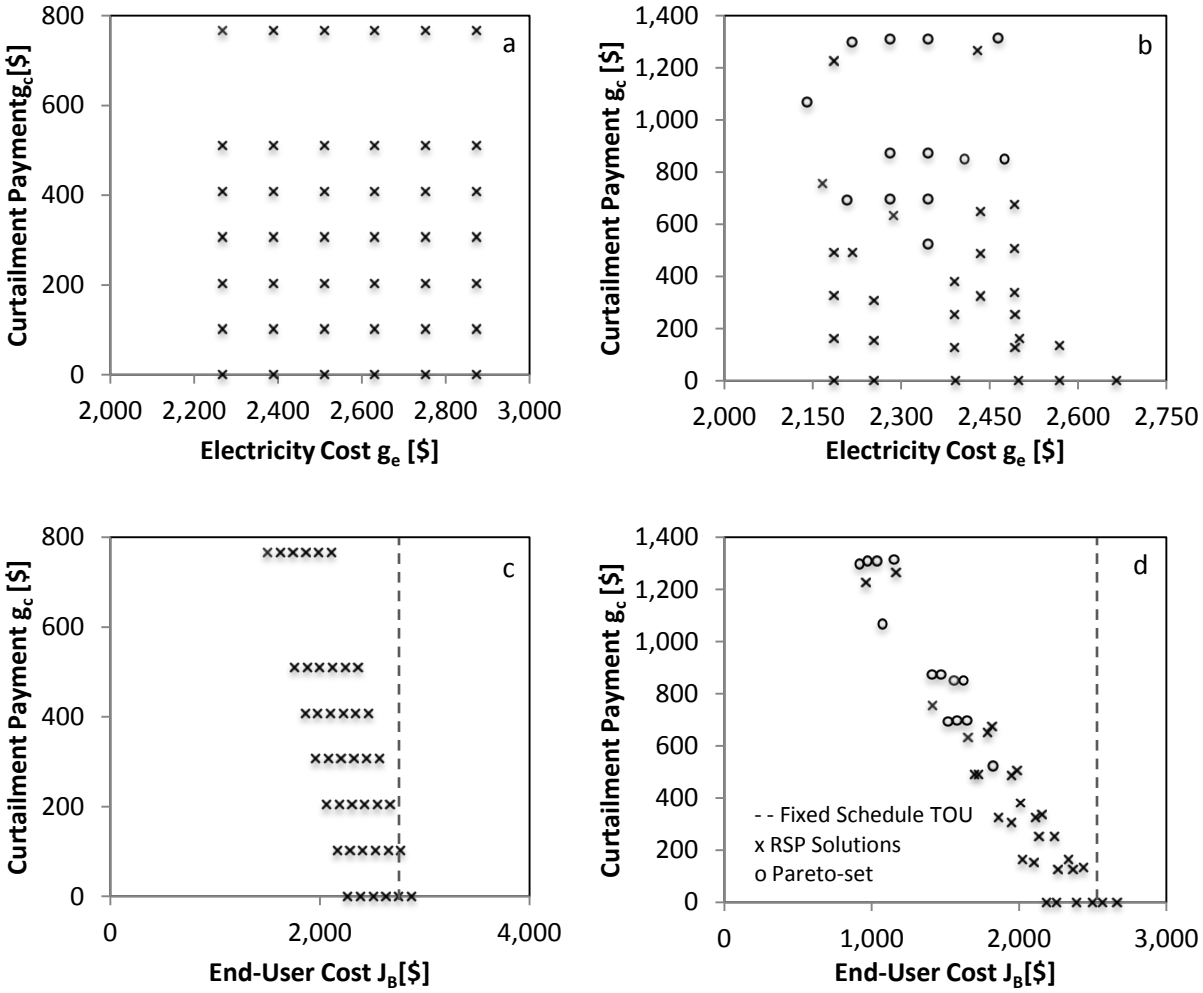

Figure 2.8 Benefit comparison for different solutions between:
a) g_e vs. g_c *Fixed Schedule CPP* b) g_e vs. g_c *Optimized Schedule*
c) J_B vs. g_c *Fixed Schedule CPP* d) J_B vs. CP *Optimized Schedule*.

First, we need to discuss the *Fixed Schedule TOU* solution. For this scenario, we have no curtailment payment and the net cost, J_B ($2436), is equal to the price of the electricity.

Next, we discuss the results for the *Fixed Schedule RSP* presented on Figure 2.8a). Here, we see that the cost of electricity is only lower than the benchmark case, shown with the dashed line, for the two lowest CPP rates. When the CP is introduced and we analyze the net cost to the end-user as seen on Figure 2.8c), we see that most solutions are now lower than the benchmark solution. In other words, without a CP plan under this scenario, most users would not be willing to switch over to a CPP/TOU rate, as it would increase their electricity expenditure.

We analyze the solutions to *Optimized Schedule RSP* using the same method. In Figure 2.8b) we see that most solutions have lower electricity cost than the benchmark case, meaning that most of these solutions would be viable even if a CP were not considered. In this graph, we also see that the Pareto-set, i.e., the set of solutions marked with 'o', achieves electricity cost, g_r, changes in the range of (-1% to 12%). Figure 2.8d) then shows the net cost to the end user compared to the curtailment payment, where most solutions achieve significantly better results than the benchmark. Here, the Pareto-set reduces the net cost to the end-user, J_B, significantly from the benchmark case (25% to 62%).

3.3 Percentage Cost Contribution

After analyzing how different factors affect the financial and operational cost to both end-users and utility, it is important to understand how much of the final end-user or utility cost can be attributed to each of these factors. To do this, we compare percentage contribution for each of the cost components to results from the *Fixed Schedule TOU*, an average solution to the *Fixed*

Schedule RSP [CPP/CP (0.6/0.6)] and an average solution to a member of the Pareto-set in the *Optimized Schedule RSP* [CPP/CP (0.2/0.8)].

3.3.1 End-User Cost

Analyzing the three contributors to the end-user cost we can determine the relative impact that each of these have on the end-user cost. Figure 2.9 shows that electricity costs is the biggest contributor to final cost for all cases, while curtailment payments, g_c, constitute 10% of the *Fixed Schedule RSP* cost and 24% of the *Optimized Schedule RSP* Pareto-set solution cost. In this figure, we also see that the occupant disutility, g_d, is negligible for all cases, with the largest contribution being under 2% for the *Optimized Schedule RSP* Pareto-set solution.

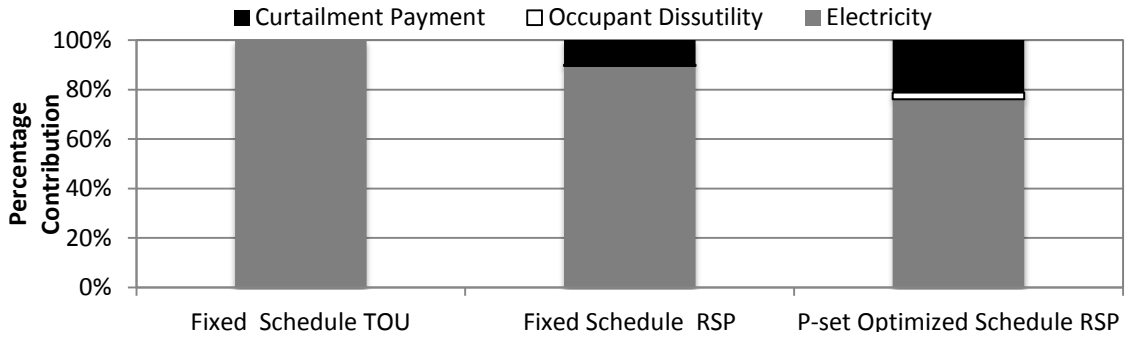

Figure 2.9 Comparison between how parameters contribute to end-user cost for the *Fixed Scheduled TOU*, *Fixed Schedule RSP*, and Pareto-set *Optimized Schedule RSP*

3.3.2 Utility Cost

After looking at the four individual contributors to the utility operation cost, we want to see how much each of these factors contributes to the final utility cost.

Figure 2.10 shows that for the *Fixed Schedule TOU* case, 49% of the utility operation cost comes from the load distribution cost, g_l, a 12% from the ramping cost, g_r, and a 39% from electricity cost, g_e. For the *Fixed Schedule RSP* 33% of the utility operation cost is contributed by the load

distribution, 30% from ramping, 4% from the curtailment payment, and 33% from the electricity cost. Finally, we see that for the Pareto-Set solution chosen of the *Optimized Schedule* we have a 31% contribution from the load distribution, g_l, a 12% from ramping, g_r, 13% from curtailment payments, g_c, and 43% from electricity cost, g_e.

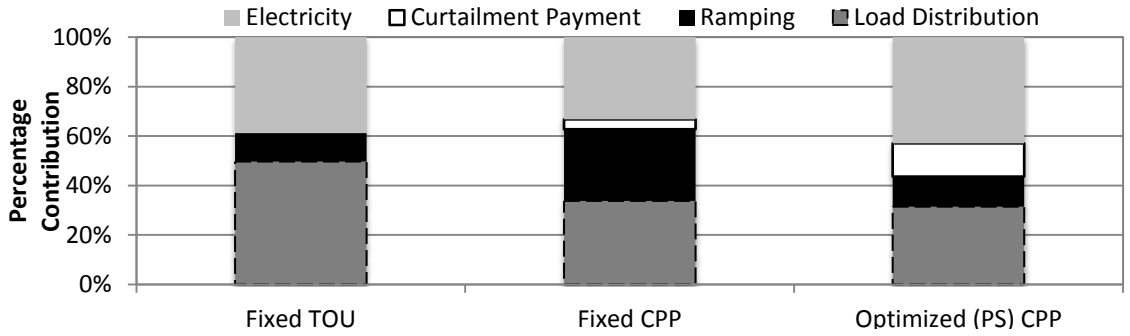

Figure 2.10 Comparison between how parameters contribute to utility operation cost for the *Fixed Scheduled TOU*, *Fixed Schedule RSP*, and *Optimized Schedule RSP*

3.4 Load Allocation

Figures 2.11a)-c) show the load profiles under each scenario for Tuesday, Wednesday, and Thursday, respectively. In each of the graphs we can see the load allocation for the *Fixed Schedule TOU*, *Fixed Schedule RSP*, and a Pareto-set solution of the *Optimized Schedule RSP* scenarios, along with the *Electricity Demand* of the building if no TES were in place. *Electricity Demand* under no TES is presented in order to highlight the benefits that TES with simple controls brings and emphasize the load curtailment potential of a TES with extra storage capacity. We analyze those graphs and compare the load distribution and stability costs for the different cases.

In each of the graphs, we use the relatively high but stable load demand of *Fixed Schedule TOU* as the benchmark to which we compare the different results. Next, we look at the *Fixed Schedule*

RSP scenario where for Tuesday and Wednesday we have significant changes in consumption at times where the *base load chiller* is turned off and back on to take advantage of CPP/CP. Thursday sees low and stable loads throughout the critical peak event hours and stays at the same level as the optimized solution. Finally, *Optimized Schedule RSP* scenario creates various load allocation solutions that are not all presented here for brevity purposes. Here, we will only present a solutions belonging to the Pareto-set, as these solutions use the same load allocation strategy during event hours, keeping a low and stable load, and are used here to represent the *Optimized Schedule RSP* scenario.

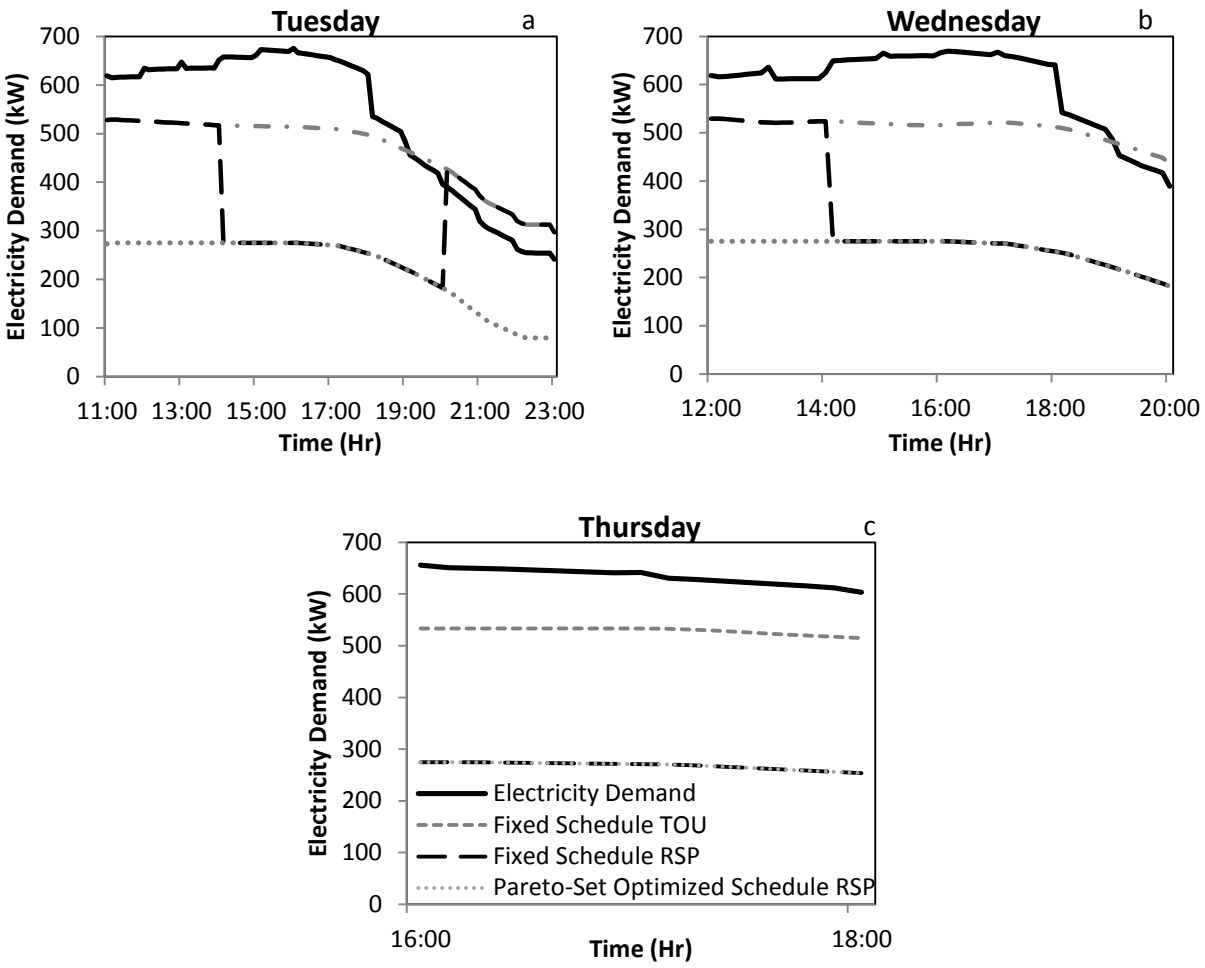

Figure 2.11 Load profile under different scenarios for a) Tuesday b) Wednesday c) Thursday

3.5 Discussion

There are several important findings out of our analysis. First, moving from the benchmark *Fixed Schedule TOU* to a *Fixed Schedule RSP* only yields attractive results to the end-user when a CP is put in place. Such a move would only bring benefits to the utility, if the load allocation and ramping cost functions were more important to utilities than what was hypothesized here. Moreover, while not every solution of the *Optimized Schedule RSP* scenario produces better results than the benchmark, we can state with confidence that a good portion of the solutions

yield better results than the benchmark for both parties involved as most cases reduce operation and monetary costs assumed by the utility and the end-user. Furthermore, the Pareto-set solution maximizes the global benefit by finding the solutions that maximize the benefit trade-offs between operation and monetary costs. This set of solutions provides the different options amongst which the utility and end-user can negotiate a desirable RSP.

A sensitivity analysis was performed in order to see how the results change after modifying the coefficients used to determine ramping and load distribution cost, c_r and c_l. We noticed that as c_r is increased, the relative benefit to the benchmark increases, while increasing c_l decreases the relative benefit. The effect is reversed if both of either one of these is decreased. Furthermore, modifying these parameters also varies the relative benefit between the Pareto-front and other solutions, but the changes are not as noticeable as they are when compared to the benchmark scenario. In this project, we use a value of $2/kW for both of these values in order to guarantee that costs to end-users and utility remain positive and are of similar magnitude.

4. Conclusion

Thermal Energy Storage (TES) has been proven to be a great tool to help reduce electricity costs by shifting building cooling load demand from time of high electricity demand to times of low electricity demand with the help of TOU rates. By creating an optimization platform where TES and rate structure package (RSP) interact, this paper explores the added benefits that can be provided to end-users and utilities. First and foremost, the platform developed here shows that the use of RSP can aid at reducing electricity demand during critical peak times, thus helping reduce capacity costs to the system. In addition, the results show that an *Optimized Schedule approach* can reduce operation and monetary costs to the utility and the end-user by optimizing

chiller operation. In particular, we find a set of optimal solutions, in the form of a Pareto-set, that minimizes global costs, reducing the electricity cost up to 12% when compared to a *Fixed Schedule TOU* benchmark, and the net-cost to end user up to 62% for one hot summer week of operation. Moreover, the operation cost function of the utility decreased by up to 48% in terms of load distribution and 14% in terms of ramping cost. Finally, the proposed framework can potentially attract more end-users to adopt RSP, thus significantly increasing the benefits of TES compared to the TOU rates only.

CHAPTER III

USING THERMAL ENERGY STORAGE TO PROVIDE SPINNING RESERVES

Abstract

With growing power system reliability concerns over the impact of extreme weather events due to human-induced climate change and the increase in deployment of intermittent renewable energy resources, the need for spinning reserves (SR) is predicted to increase in the coming decades. Furthermore, with the current goals of decreasing dependence on fossil-based resources, the need for demand-side resource capable of providing spinning reserves has significantly increased. In particular, there has been great interest in how these services can be provided by controlling cooling demand, through direct control of a building's temperature. This paper develops a new method along with a simulation platform to allow building managers to respond to spinning reserve calls without sacrificing occupant comfort. This is accomplished through the innovative use of a thermal energy storage (TES) system that can curtail all of a building's flexible cooling load during deployment times. Moreover, this paper quantifies the financial benefits to a building manager of using the TES to provide spinning reserves. Through this analysis we show that most of the benefits stem from the capacity payments for resource availability as opposed to actual load curtailment. Finally, we conclude that the implementation of such a system is technically feasible, economically attractive, and results in no occupant discomfort.

Terminology

AS Ancillary Services

FERC Federal Electricity Reliability Commission

NYISO New York Independent System Operator

ISO Independent System Operator

RTO Regional Transmission Organization

TES Thermal Energy Storage

DA Day-ahead

RT Real-time

SR Spinning reserve

1. Introduction

As power systems integrate more intermittent renewable resources, and as the changing climate increases the number of days with extreme heat, the need for spinning reserves will continue to grow. Spinning reserves are reliability resources that can quickly adjust their power output in response to network contingencies such as line or generator failures, or to rapid changes in renewable generation. In almost all North American power systems, spinning reserves are provided by natural gas and hydroelectric generators. One possible way to meet the growing need for spinning reserves is to allow demand-side participants to compete in spinning reserve markets.

In recent years, several system operators have begun exploring this possibility. This trend is due in part to experiments such as[78,79], which have demonstrated the feasibility of providing spinning reserves by turning off air conditioners. While this approach is fast and scalable, it runs the risk

of inconveniencing building occupants by letting temperatures drift outside the range of comfort. This concern is particularly important in commercial buildings, where the productivity of building occupants is a far more valuable than spinning reserve revenues.

An alternate approach, so far unexplored in the literature, is to provide cooling from thermal storage during spinning reserve deployments. If feasible, this approach would have the advantage of maintaining occupant thermal comfort, even during deployments. Thermal storage is a mature technology that has been used for decades to shift commercial buildings' cooling loads away from times of high electricity prices. A typical (cold) thermal storage system consists of one chiller that directly meets load, another chiller that makes ice, and an insulated storage tank. Such systems are typically operated with heuristic schemes like chiller priority, storage priority, or constant proportion control. In recent years, however, various researchers have applied model predictive control to thermal storage, with encouraging results[22,54]. For a precise and readable comparison between model predictive control and these heuristics, see Henze et al.[22]

While model predictive control of thermal storage has shown promise, there are barriers to its uptake in industry. Perhaps most importantly, facilities engineers seldom have experience with model predictive control, and are understandably reluctant to discard working systems in favor of an unfamiliar technology. Another barrier is the fact that many buildings have insufficient automation to enable model predictable control.

In this paper, we propose an optimization-based thermal storage control scheme that is easier to intuit and implement than model predictive control, but more readily adapted to spinning reserve markets than the heuristics mentioned above. We restrict attention to three modes of operation: (1) ice-making, where the base chiller provides cooling and the ice chiller makes ice; (2) ice-

thawing, where cooling is provided from both the base chiller and from melting ice; and (3) spinning reserves deployment, where the main chiller is turned off and all load is met by melting ice. This reduces the control problem to deciding on the mode of operation at each time step.

The simulations are performed in TRNSYS, a commercial software package that solves transient heat flow equations, with the cost functions evaluated along with the building simulation. We argue that this control scheme is both sufficiently simple and -- due to its use of a detailed physical model of the building, rather than the simplified mathematical models employed in model predictive control -- sufficiently grounded in reality to be appealing to working facilities engineers.

For the purposes of this paper, we will analyze the NYISO market, focusing on the 10-min spinning reserve (SR) because of their high market value[80–83].

This paper is organized as follows. In Section 1, we briefly introduce the market operations of the New York Independent System Operator (NYISO), a representative of North American system operator. In Section 2, we describe the NYISO spinning reserve market in detail. In Section 3, we discuss recent changes in renewable integration and extreme weather events in New York State, as well as the implications for the future of NYISO's spinning reserve market. In Section 4, we discuss the physical, financial aspects of our model. In Section 5, we discuss the following results: (1) that 10-minute spinning reserve provision through thermal storage is technically feasible; (2) that it appears economically attractive; and (3) that it can be done with no inconvenience to building occupants.

2. Spinning Reserves

2.1 Minimum Spinning Reserve Requirement

The main role of SR is to ensure the reliability of the electric system in the case of a contingency, where load serving entities need to provide a minimum number of reserves in proportion to their loads. The NYISO 10-min SR requirement is required to equal or exceed the largest possible contingency[84]. This requirement increased from 600 MW in 2011 to 655 MW in 2012[81], following an increase in the system's largest generator[81].

2.2 NYISO Spinning Reserves Market Operation

The NYISO spinning reserve market settles on the day-ahead (DA) and real-time (RT) markets and it is it co-optimized with the energy market[82], making it challenging for demand-side resources to provide spinning reserves, as their bids can be accepted by the energy market, committing them to providing resources for longer periods of time that they are capable of. In order to address this problem, FERC is in the process of analyzing current procedures to make sure that market operation does not have a bias against demand-side and storage resources[82] .

The market settles in the following manner. In the DA reserves market, resources can bid in by providing their availability and amount of power they can provide. The market operator then determines which reserves to accept based on their minimum reserve requirements and predicted demand for the next day. During the DA market, a great majority of hours will have a non-zero settling price, as resources are committed to provide their services. As the day of operation progresses, the ISO/RTO can adjust the DA offers and schedules based on RT information and current projections to ensure system reliability. If during the RT, the ISO/RTO determines that it

needs more reserves, it will accept bids from available resources, and will thus post non-zero settling prices in the RT SR market.

2.3 Reserve Shortage

As demand for resources to provide energy and/or spinning reserves services increase, availability of inexpensive resources to provide spinning reserves will decrease, forcing the system to use more expensive resources, causing the price of spinning reserves to increase. Once the marginal cost of scheduling a reserve increases beyond the "demand curve" set by the different market operators for their reserves, $500/MW in NYISO, the market is unable to schedule the minimum operation reserves requirement, and a reserve shortage occurs [81]. These types of events reduce system reliability, as insufficient amount of reserves are available to support the grid in the case of a contingency.

2.3 Reserve Deployment

In order to understand deployment frequency and deployment duration for the region of interest, it was necessary to analyze NYISO historical data for SR deployment between 2001-2013[85]. Using this data, we found that reserves were deployed an average of 243 times with a standard deviation of 92 instances, where the maximum deployment instances occurred in 2007 at 438 instances and the minimum occurred on 2011 with 126 deployment instances, as seen on Figure 3.1a. Furthermore, the data analyzed showed that all deployments tend to be short as shown on Figure 3.1b, where the average and median historical deployment durations were 7.2 and 6.8 min, respectively, with a standard deviation of 5.8 min. Here, it is important to note that there were 12, 8, and 3 instances not shown on Figure 3.1b, where deployment duration exceeded 30,60, and 90 min, respectively.

Analyzing the reserve deployment data we discover that the likelihood of reserves scheduled on the DA or RT market to be deployed has decreased in the last four years, where four-year averages have steadily decreased since 2009 at an average rate of 16% per year. Furthermore, if we assume that reserves could only be deployed once every hour, something that is not necessarily true, we find that reserves are on average deployed 2.77% of available time-slots in a year. Moreover, we also find that 75% and 98% of all deployment instances have durations shorter than 10 and 15 min, respectively. Through this analysis of historical NYISO data, we can infer that future reserves scheduled on the DA or RT markets will have short duration and will be rarely deployed.

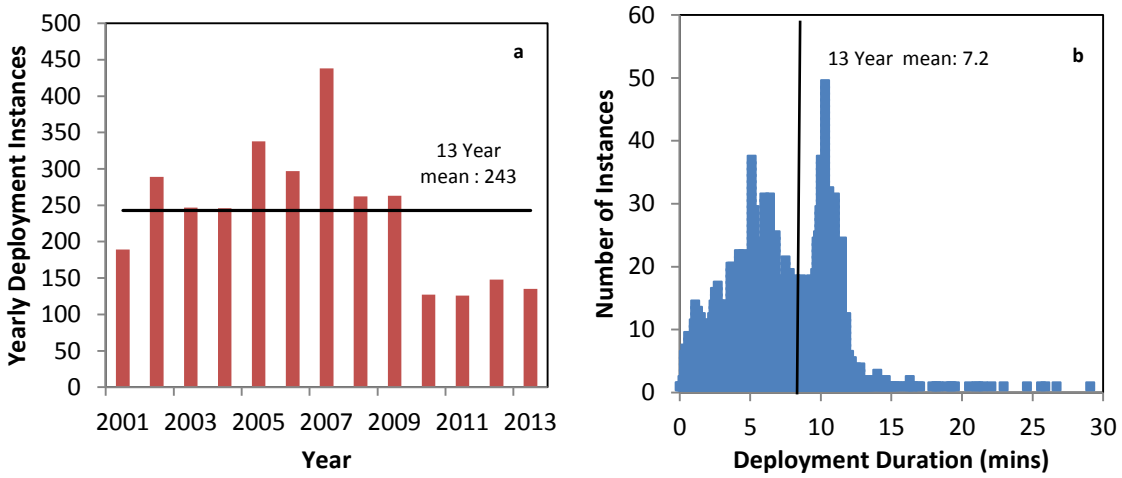

Figure 3.1 Historical SR deployment for 2001-2013 to show a) yearly deployment instances b) number of deployment instances based on deployment duration

3. Changing Weather and Renewable Energy Patterns

Uncertainty and variability of electricity demand and renewable energy generation has a great impact on the availability of resources to provide SR. Here, we set out to explore the roles that

increasingly frequent extreme weather events and increasing dependence on intermittent wind resources may play in determining operating reserve commitments and reserve shortages.

3.1 Changing Weather Patterns

The frequency and severity of extreme weather events in the northern hemisphere has significantly increased[1–6] as a result of human-induced climate change. Moreover, it has been reported that the frequency and severity of events will continue to increase in coming decades[2], so that by mid-century, well over 50% of summer days in the U.S. will experience extreme temperatures[4], with the frequency of heat extremes expected to increase seven-fold by 2040[1].

If we are to consider a scenario where climate change increases the frequency of extreme weather events during the summer, or heat waves, we must consider its implications on the electricity sector. With increasing summer temperatures, the amount of cooling required by buildings is expected to increase, thus increasing overall electricity consumption[7,8]. More importantly, increases in maximum daily temperatures will significantly increase peak electricity demand[9], increasing system requirements for additional capacity and reserve resources, as well as reducing the amount of resources capable of providing those services.

Using historical electricity consumption[86] and 10-min SR data from NYISO[87], we seek to understand the effect increasing peak load demand has on spinning reserve shortage. To do this, we first compare the number of reserve shortage instances with the number of times electricity demand in NYC exceeds a high load level, 10.5 GW, for June, July, and August for the years 2007-2013, as shown on Figure 3.2a as a time-series. Figure 3.2b then shows the data as scatter diagram with a linear regression and a coefficient of determination of $r^2 = 0.385$, with normally

distributed residuals. Here, we see that, in general, as the number of instances the load in NYC exceeds 10.5 GW increases, so do the number of reserve shortages that occur within that month.

The correlation coefficient between the two data sets is r=0.62 with n=21 data points. We use a one-tailed hypothesis test with a standard α=0.05, where we make use of a null hypothesis that states that the two data sets are not correlated, or are negatively correlated, and an alternate hypothesis that states that there is a positive correlation between peak load in NYC and the number of SR shortages. We find that the test statistic, t=3.417, and the p-value=0.0014. Because the p-value< α, we are able to reject the null hypothesis, and conclude that there is a non-zero correlation between the two sets of data.

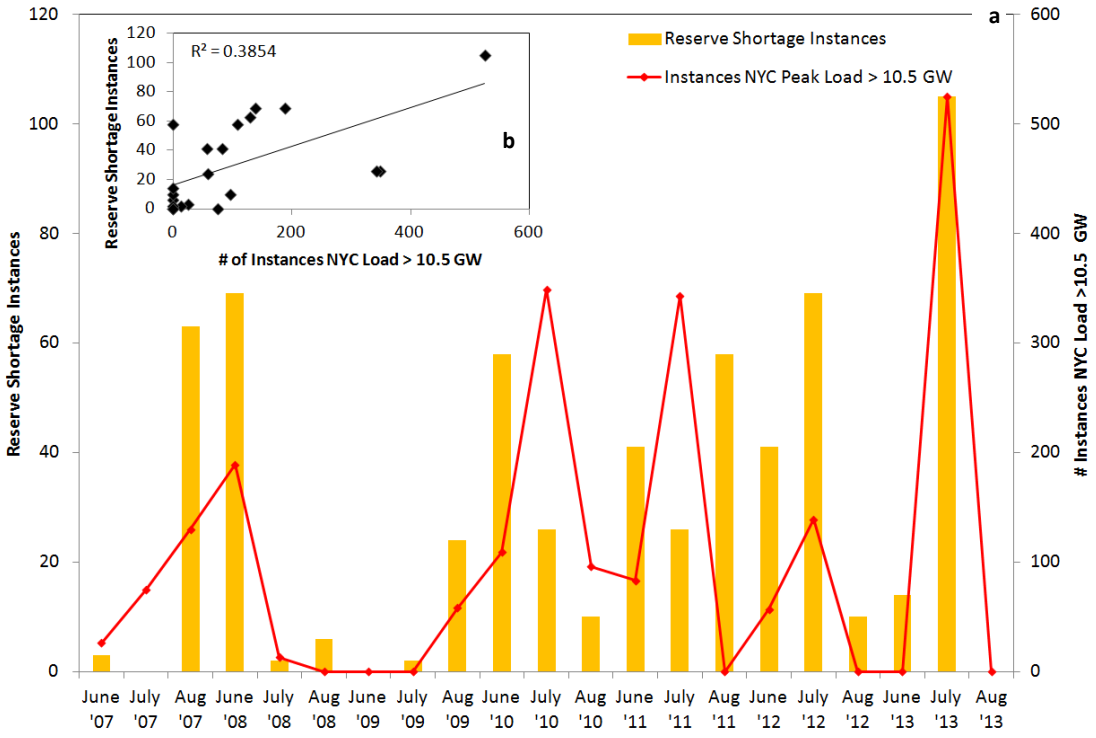

Figure 3.2 Historical NYC summer peak load and number of 5-min summer SR shortages shown in a) a time-series and b) a scatter diagram with a regression line

Analyzing the figures and the hypothesis test, we can say that, for the months studied, summer peak load and shortage of SR are correlated, even if only slightly. This correlation could be explained in the following way. As temperatures and electricity demand soar, cheap and medium-price resources that provide energy and ancillary services will be committed first, leaving only the expensive resources available to provide spinning reserves in the RT market, thus increasing the likelihood of a SR shortage. As long as traditional generators dominate the AS market, the likelihood of SR shortage will be higher during peak demand times.

Despite the results presented and discussed here, it is important to keep in mind that these are general results and if we wish to better understand the effects of increasing electricity loads on SR shortage, more in-depth studies are needed.

3.2 Wind Generation Intermittency & Growth

In the last decade, wind power has been one of the fastest growing generation technologies in the U.S., reaching an installed capacity of 61 GW by the end of 2013[88] and the Rocky Mountain Institute projects that it could increase up to 580 GW by 2050[89].

As wind becomes a significant source of electricity for the U.S., concerns over the effects of wind intermittency on system reliability have grown, prompting many wind integration studies[90–99]. With respect to spinning reserves, the biggest finding from comparing the different studies is that the level of spinning reserves needed to accommodate higher wind penetrations is not a constant function of installed capacity[96]. Moreover, these studies also showed that while wind might not need to be considered a contingency to the system, it does require activation and deactivation of additional spinning reserves in order to account for short-term output

variability[96]. Furthermore, short-term wind variability could also be responsible for an increase in frequency of SR shortages in systems with large wind penetration[100].

3.3 Effects on Spinning Reserves

Although the exact effect of climate change and increasing wind power penetration will have on operating reserve requirements shortages cannot be exactly determined from the different studies and data shown here, to ensure reliability under these scenarios, the electric system needs to find ways to effectively respond to short-term changes in generation while keeping the costs of electricity from rising significantly. This can be achieved by developing new methods for demand-side resources to participate in the ancillary services market and through the creation of policies to encourage demand-side resource participation.

4. Using TES to provide Demand-side Spinning Reserves

Using some of the market principles outlined in section 2, we now wish to build a platform to investigate how an individual building would operate in the NYISO 10-min SR market using TES and what their potential benefit of doing this would be. In order to simplify the problem, we assume that a building manager would only participate in the DA SR market. This assumption leads to a conservative estimate of the potential benefits, as the payments for participating in the RT market tend to be much higher.

In order to estimate the potential benefit to the end-user, we study the month of July, 2013, dividing it into four 5-day periods in order to see weekly performance variability for this period.

We will first describe basic TES operation, moving on to describing the platform where a physical and financial model interact to simulate operation and economic implications for a building operator of participate in the SR market.

4.1 Platform

The system consists of a physical model and a financial model, coupled by a decision platform that operates in a TRNSYS simulation platform, as shown by Figure 3.3. The physical model represents the building and the HVAC system; the financial model contains information on rate schedule, DA SR settling prices and wholesale electricity prices. The decision platform, which contains information regarding commitment and deployment schedule, uses scheduling variables to operate the HVAC system and determine the total costs associated with this particular scheduling constraint.

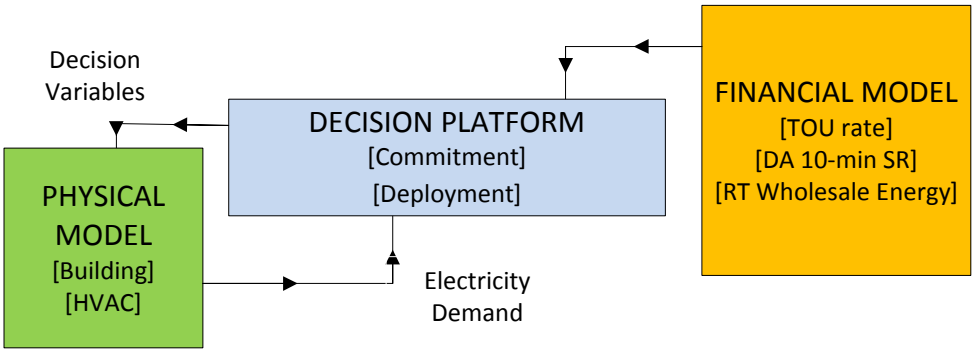

Figure 3.3 Components of the simulation platform

4.2 Physical Model

The physical model on the optimization platform consists of a building, an ice storage tank, and a two-chiller system. The following sections describe how each of these components was modeled.

4.2.1 Building Model

The modeled building used in this study follows the ASHRAE 90.1 Prototype Building standards[59], which reflects a typical air-conditioned new construction 3-story 153,000 sq-ft office building. A simplified building model for this ASHRAE building is available in the TESS libraries in TRNSYS[60]. This model was modified for this study in order to account for the internal gains of the building and to incorporate an HVAC system in accordance with ASHRAE standards. Schedules for building use and occupancy vary on a diurnal schedule, peaking during normal business hours.

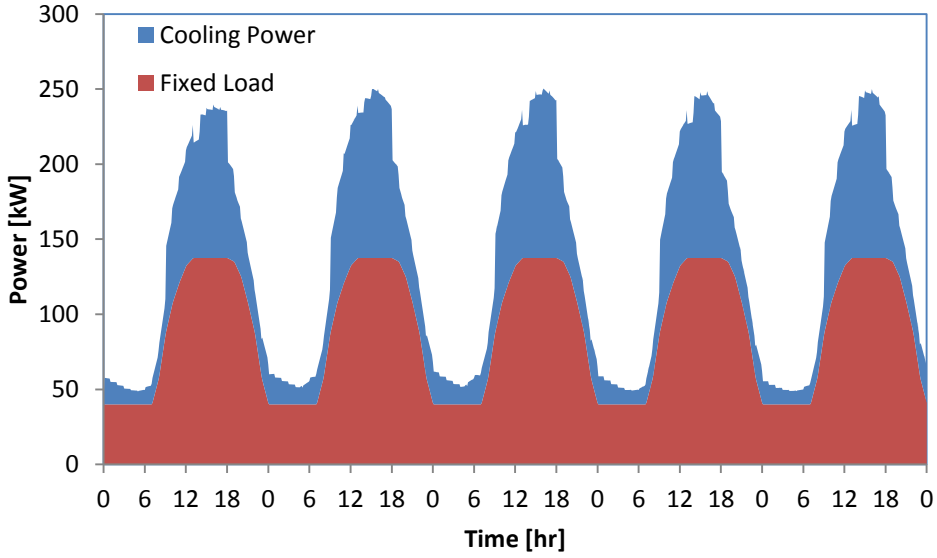

Figure 3.4 Buildings' fixed and cooling Load for a 5-day period

The model developed here simulates the cooling that the building needs in order to maintain the thermal comfort in each thermal zone, as specified by ASHRAE standards. Figure 3.4 depicts the variation between day/night cooling power demands for this building for five summer days. Total electricity demand for the building is then obtained by estimating the standard *fixed load*

electricity consumption profile for lighting, plug-loads, and ventilation systems[62–65], and adding them to the electricity consumption associated with cooling demand. The stacked *fixed load* and *cooling power* for the building are shown on Figure 3.4, also giving us an idea of what the electricity demand for the building would be if no TES were used.

4.2.2 Cooling System

The cooling system described here consists of a two-chiller system to maintain a good system efficiency and reduce chiller sizing needs[23]. As a result, the system has two separate loops: the glycol mixture loop for ice making and the water loop that provides continuous cooling load to the building. This system operates in three different modes: ice-making/charging, ice-thawing/discharging, and SR deployment.

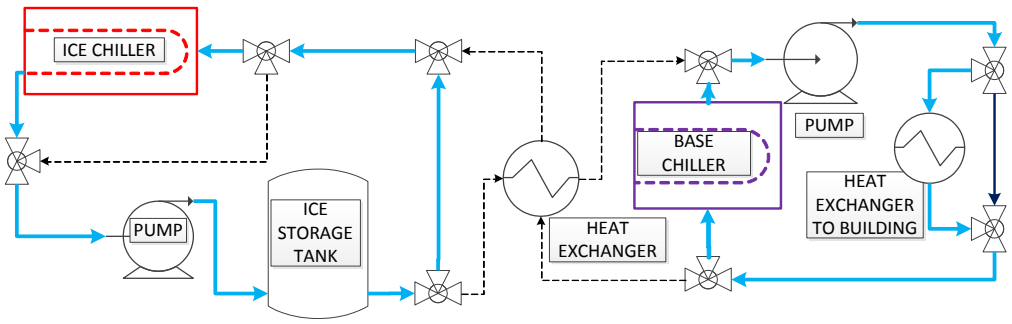

Figure 3.5 The ice-making mode of operation

The ice-making mode, shown in Figure 3.5, consists of both the glycol and the water loop running independently of each other. The glycol loop is used to transfer cooling load from the *ice chiller* to the ice storage tank, thus making ice, while the water loop is used to provide direct cooling needs to the building. This mode is exclusively used during times when the *base load chiller* can provide all of the cooling needs of the building, which, given cooling demand patterns, happens only during the night and early morning.

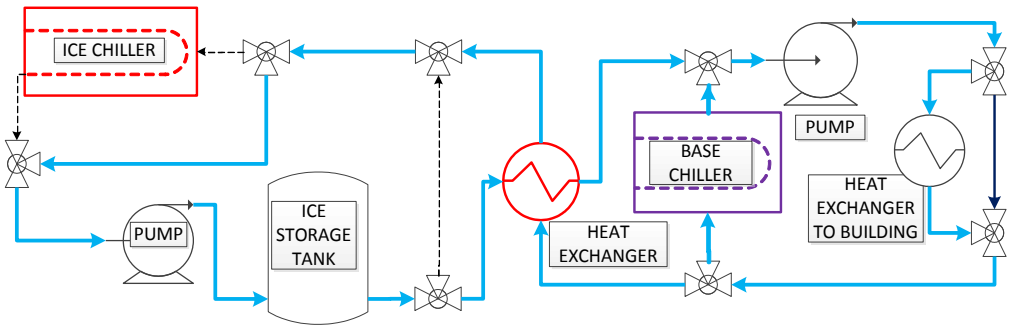

Figure 3.6 The ice-thawing mode of operation

The ice-thawing mode, shown in Figure 3.6, operates when the glycol loop is connected to the water loop via a heat exchanger in order to supplement the cooling load. As the heat transfer between the water and glycol loop takes place, the amount of ice available in the storage tank decreases. The discharging mode takes place at times when the *base load chiller* alone does not have the capacity to provide all of the cooling needs of the building. During these times, the *base load chiller* runs at full capacity; providing 30% to 40% of the peak cooling load. This mode is used during late morning to early evenings, where cooling demand is highest.

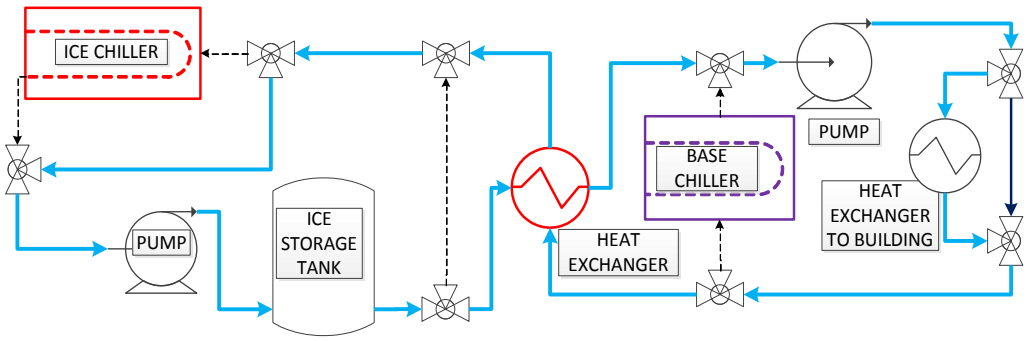

Figure 3.7 The spinning reserve deployment mode of operation

Spinning reserve deployment is a mode of operation that can be used in order to respond to deployment calls, as shown in Figure 3.7. This mode functions by turning off the *base load*

chiller and providing all of the cooling load through the ice storage tank, thus significantly reducing power demand and complying with SR commitment.

4.2.3 Chillers

The cooling system uses two air-source chillers in order to provide the necessary cooling load. The *base load chiller* uses water as a refrigerant and operates at a temperature of 3°C with a rated COP of 3.6. The *ice chiller* uses glycol as a refrigerant, operates at a temperature of -6.67°C, and has a rated COP of 2.8. Performance data for both chillers were obtained from chiller data sheets for a TRANE chillers[66]. The *base load chiller* and *ice chiller* are sized at 75 and 75 tons (of refrigeration), drawing 72 and 93 kW, respectively.

4.2.4 Ice Storage Tank

The ICEPIT ice storage tank developed by Hornberger[68] was used for the TRNSYS implementation of the TES. The parameters for the ICEPIT were obtained following the ICEPIT validation presented by Christophe and Philippe[69].

4.3 Financial Model

The financial model is used to provide the platform with the different financial information needed to operate. This part of the model contains the TOU electricity rate, the DA SR prices, as well as the wholesale RT electricity prices.

4.3.1 TOU Rate

A hypothetical 3-tiered TOU rate was used as shown in Figure 3.8 where the on-peak price is $0.23/kWh, the medium-peak price is $0.19/kWh and the off-peak price is $0.063/kWh. Here,

we only consider energy prices, as the maximum demand for the summer is not expected to change when compared to typical TES operation, thus a demand charge would have no effect on the final end-user electricity cost.

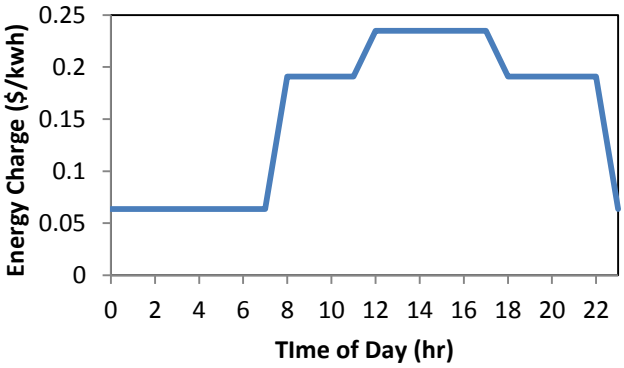

Figure 3.8 Daily 3-tiered TOU pricing used

4.3.2 Energy Cost

Let $P \in \mathbb{R}^{24\times7}$ be a matrix containing the average power consumption P_{ij}(kW) during the i^{th} hour of the j^{th}day for a 5-weekday period. Then the electricity cost ($) is

$$g_e(P) = \sum_{j=1}^{5}\sum_{i=1}^{24} c_{ij}P_{ij}\Delta t$$

where c_{ij} ($/kWh) represents the energy charge during hour *i* of day *j*.

4.3.3 Spinning Reserve Commitment

Given the type of building described here, cooling load demand is low and variable during off-peak hours, making it challenging to find the best strategy to place bids during times where capacity payments are low and spinning reserve deployments happen regularly. For this reason,

we limit the periods when SR can be provided to on-peak times when the *base load chiller* is operating at full capacity. Moreover, SR commitment in the RT market would require constant human supervision or an extremely advanced control system. For this reason, we do not consider the possibility of offering up resources in the RT market. Through these assumptions, we are proposing an easy to use system that significantly underestimates the value that such a system could bring to the end-user.

In order to successfully bid on the SR market, the building manager predicts the amount of power the building can curtail by turning the *base load chiller* off and bids this in the DA SR market. For our purposes, we assume the building manager can easily and accurately predict cooling demand in a 5-day horizon, and bids accordingly.

For the case described here, the building manager sends weekly offers B_{ij} (kW-hr) by using the following formula.

$$B_{ij}(P) = \prod_{j=1}^{5} \prod_{i=1}^{24} z_{ij} b_{ij}$$

where b_{ij}(kW-hr) represent the amount of power the building can provide as reserves for a one-hour period, and z_{ij} is a binary function of the form

$$12 \leq i \leq 19 \qquad z_{ij} = 1$$

$$else \qquad z_{ij} = 0$$

where 12-19 represent the hours when the base-load chiller is operating at full capacity and thus capable of providing a significant amount of SR.

4.3.4 Spinning Reserve Capacity Payment

Current practice does not award opportunity costs to demand-side resources for providing ancillary services. Given this, we can assume that the building behaves as a price-taker and their bid will be accepted at the closing price for the market. So for any of the bids accepted to provide spinning reserves, the payment made to the building manager, $p_{DA}(P)$ ($), is determined using the closing market price for the DA SR, DA_{ij} ($/kW-hr).

$$p_{DA}(P) = \sum_{j=1}^{5} \sum_{i=1}^{24} DA_{ij} B_{ij}$$

Moreover, because demand-side resources are relatively cheap and to simplify the problem, we will assume that all bids will be accepted.

4.3.5 RT Deployment Payment

Whenever the grid-operator deploys a SR resource that has been committed on the DA (or RT) market, the grid-operator must make a payment, $p_{RT}(P)$ ($), to the resource for the amount of energy provided (curtailed) based on the wholesale energy price.

$$p_{RT}(P) = \sum_{j=1}^{5} \sum_{i=1}^{24} RT_{ij} C_{ij}$$

where C_{ij} (kW-hr) is the amount of load deployed, curtailed, by the demand-side resource in accordance to their DA bid and RT_{ij} ($/kW-hr) is the RT wholesale energy spot-price.

4.3.6 RT Deployment

Table 3.1 Spinning Reserve Deployment for weekdays July 2013

Deployment Duration (min)

	Monday	Tuesday	Wednesday	Thursday	Friday
Week 1			7.5		15
Week 2			15	15	
Week 3	21	21	7.5	7.5	
Week 4		15	7.5		

To test the platform presented here, we used historical NYISO SR deployment data (as discussed on section 2.4) for the month of July in 2013 [85] as shown on Table 3.1, for reference. In this table days with a SR deployment are marked by the duration of the event, where the actual duration is rounded up to match the simulation step-times.

4.4 Results

In order to show that demand-side resources can provide SR services, we discuss the operation and financial effects of responding to a SR deployment call.

4.4.1 Chiller Operation

Chiller operation varies slightly from operation under a standard TES strategy as shown in Figure 3.9a, where the *ice chiller* is only turned on at night in order to take advantage of off-peak prices, while the *base load chiller* operates throughout the day and is turned off only to respond to a SR deployment. Figure 3.9b, shows a close-up of the SR call and power consumption before,

during, and after the deployment call, where we can see the reaction time for the chiller to turn off and to turn back on. Figure 3.9c, then shows the total daily building power consumption. Here, we see that chiller load is quite high during the night, when both base load and ice chiller are in operation.

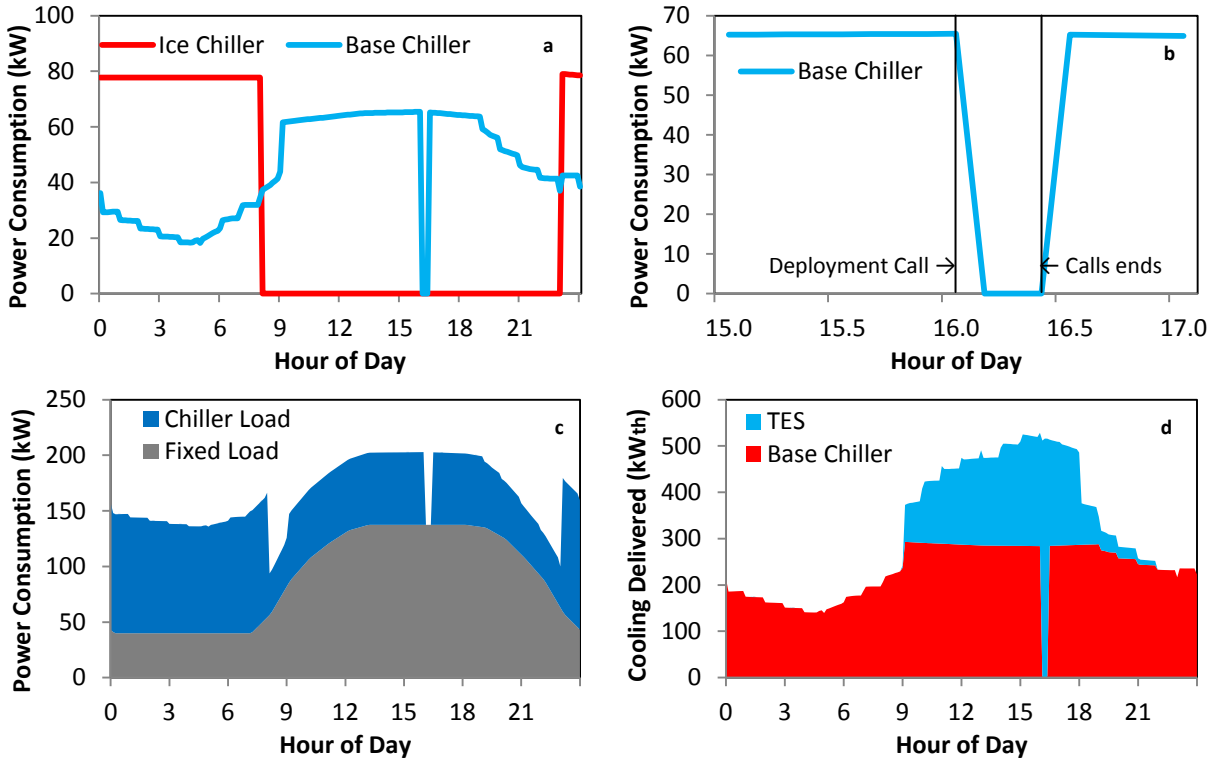

Figure 3.9 Daily profiles for Wednesday July 17th, 2013 for a) ice and base-load chiller power consumption b) base-load chiller reaction c) total building power consumption d) thermal load delivered by the base-load chiller and the TES

Finally, Figure 3.9d shows how the TES provides cooling demand during peak hours of the day, increasing cooling output during the SR call in order to meet the cooling deficit from turning the *base load chiller* off. These results show that, if properly operated, a building with TES could be capable of providing 10-min SR services.

4.4.2 Financial Implications

In order to assess the financial benefit that demand-side resources with TES could obtain, we compared each of the weeks being studied with results where the building does not participate in the SR market. The results comparing the end-user cost when participating in the SR market, *Net Cost with SR*, with the corresponding benchmark scenarios, *Net Cost w/o SR*, are shown in Figure 3.10a. Here, we see that participating in the SR market could signify a net-cost reduction to the end-user of $30/week thanks to capacity and deployment payments made by the utility provider, as well as some energy savings during the deployment event. Moreover, Figure 3.10b shows the payments made to the end-user by committing and deployment 10-min SR, where capacity payments significantly outweighed deployment payments, with the exception of the third week, when four out of the five days experienced deployment events. Also, we can see here that the energy savings are minimal for every week. Finally, the savings obtained through capacity and deployment payments, as well as the energy savings, are divided by the weekly net cost without SR to represent the percentage savings that operating under such a system would bring to the building operator as shown in Figure 3.10c. Here, we see that just from the capacity payment, the building operator would incur >4% savings on their electric bill with those reductions increasing up to 10% in weeks with numerous deployment events. These results show that the financial incentives of providing 10-min SR services are quite attractive even under a scenario with few deployment events.

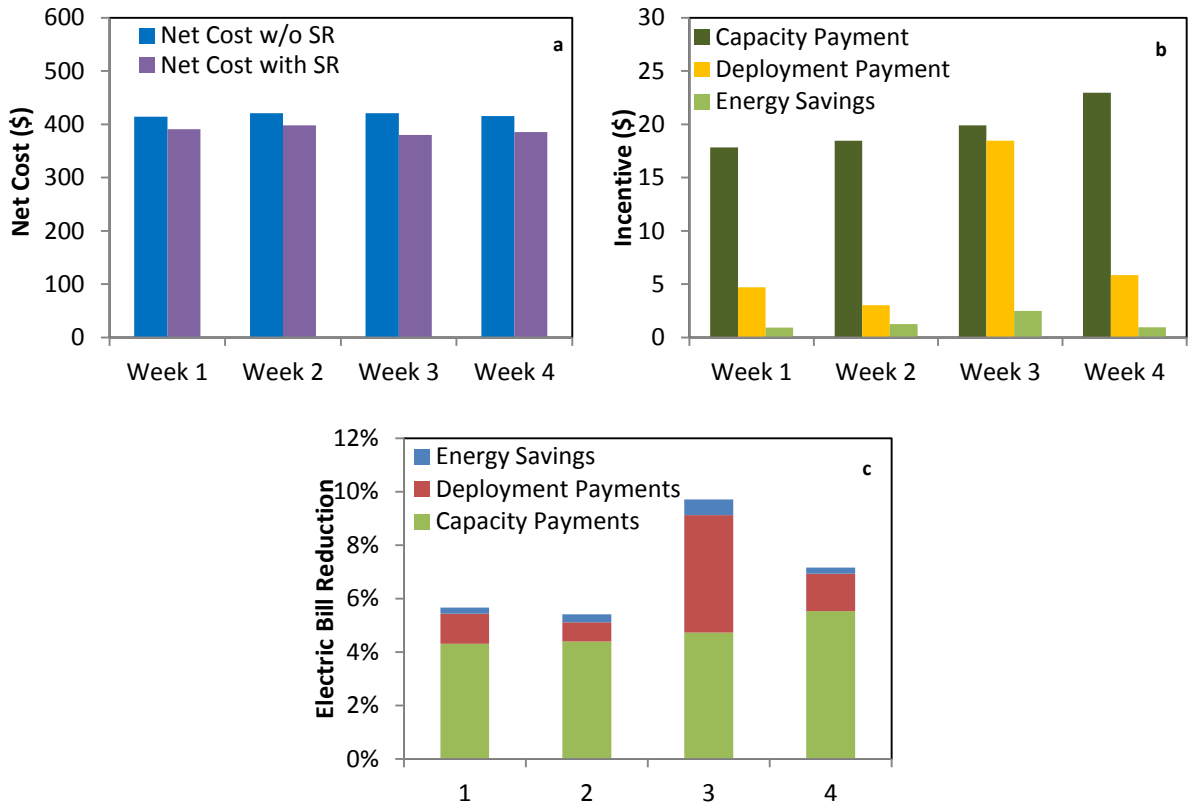

Figure 3.10 a) Weekly comparison between the net cost without providing SR and providing SR, b) weekly monetary incentive from energy savings, capacity payments, and deployment payments and c) weekly percentage savings stemming from energy savings, capacity payments and deployment payments

4.4.3 Discussion

After analyzing the benefits that building operators could obtain from participating in the 10-min SR market, it is important to discuss some practical considerations in employing TES on the ancillary services market, as well as to discuss the impact that such a move could have on the entire grid.

To successfully operate a TES mechanism to provide 10-min SR, the following system aspects need to be considered. In order to respond to deployment calls, the TES should have an automated control system capable of controlling chiller operation without human input. Moreover, the base-chiller should be capable of rapidly responding to a deployment call as well

as rapidly coming back online after the call has ended. Finally, the tank size of the TES needs to be slightly oversized when compared to a traditional system, in order to provide the additional cooling requirement during deployment events. For the simulations presented here, only a 5% increase in storage capacity was needed to provide reliable service during deployment calls.

The potential TES impact on the electric grid is the following. First, by allowing medium-sized buildings to curtail all of their cooling load for a short amount of period, the number of resources needed to provide spinning reserves could be decreased, making the process easier to manage and control. It follows that in the short to medium-term, demand-side resources can play a significant role in the ancillary services market by providing large amounts of spinning reserves at a low marginal cost. In the case of TES, technology and utility incentives have made it economically viable for many medium and large commercial buildings to install TES in order to reduce their energy consumption; systems that can in addition be used to provide ancillary services such as 10-min SR as outlined in this paper.

In the coming decades, increasing environmental concerns over pollution and climate change resulting from inefficient generators with fossil fuels[101], may outweigh the benefits of using peaking generators[101,102] to provide spinning reserves, and in turn incentivize the usage of more diverse resources to provide SR.

5. Conclusion

Spinning reserves play an important role in electricity grids, a role that will likely be magnified over the coming decades due to increasingly frequent extreme weather events as well as an increase in intermittent energy sources. It is important to find ways in which existing technology can be used in order to increase the number of resources capable of providing spinning reserves,

and if necessary from deploying their resources in real-time. This paper describes the challenges that the electric grid faces, and outlines a method through which demand-side resources could make use of TES in order to provide spinning reserves services, while also obtaining financial benefits. These resources could expect savings ranging from 5% all the way to 10% of their electricity expenditures through capacity and deployment payments.

MAJOR CONTRIBUTIONS

The primary contributions of this thesis center around developing new platforms for TES implementation and quantifying the technical and economic benefits that can be achieved through innovative use of thermal energy storage (TES), where end-users gain financial benefits and the power system benefits through improved performance and a reduction in operation and capacity costs.

In this thesis, I showed that the aggregation and planned allocation of flexible cooling loads through TES can reduce power system operation costs by reducing peak usage and flattening out the load profile. Moreover, I showed that by optimally allocating cooling loads, the power system can increase its load factor, reduce peak to valley ratio and reduce system ramping; factors that improve system performance and make the operation planning process easier. Furthermore, I showed a reduction in capacity payments as a result of peak load reduction.

In addition, I have developed a practical simulation platform for optimal operation of TES that allows building managers to add functionality to traditional TES systems without the need for in-depth understanding of various advanced control methods.

My work on using TES to provide demand-side management services and spinning reserves highlights truly innovative TES applications that provide added benefits to both end-users and the power system. The added financial benefits to end-users help reduce TES payback period, making TES a much more attractive investment, while the power system benefits by having cheaper resources available to provide spinning reserves as well as lowering peak demand and capacity costs through the use of dynamic pricing mechanisms. Furthermore, this work showed the value of implementing suitable dynamic electricity rates and demand-side management

curtailment payments encourage program acceptance, to maximize participation during critical peak events, to maximize the benefits to end-users and the power system.

REFERENCES

(1) Coumou, D.; Robinson, A. Historic and future increase in the global land area affected by monthly heat extremes. *Environmental Research Letters* **2013**, *8*, 034018.

(2) Rahmsotrf, S.; Coumou, D. Increase of Extreme Events in a Warming World. *Proceedings of the National Academy of Sciences* **2012**, *109*, 4708–4708.

(3) Jones, G.; Stott, P.; Christidis, N. Human contribution to rapidly increasing frequency of very warm Northern Hemisphere summers. *Journal of Geophysical Research* **2008**, *113*, D02109.

(4) Duffy, P. B.; Tebaldi, C. Increasing prevalence of extreme summer temperatures in the U.S. *Climatic Change* **2012**, *111*, 487–495.

(5) Petoukhov, V.; Rahmstorf, S. Quasiresonant amplification of planetary waves and recent Northern Hemisphere weather extremes. *Proceedings of the National Academy of Sciences of the Unidted States of America* **2013**.

(6) Climate Communication: Science & Outreach. Heat Waves: The Details http://www.climatecommunication.org/new/articles/heat-waves-and-climate-change/heat-waves-the-details/#refmark-5 (accessed Apr 16, 2014).

(7) Lam, J. Climatic and economic influences on residential electricity consumption. *Energy Conversion and Management* **1998**, *39*, 623–629.

(8) Sailor, D. J. Relating residential and commercial sector electricity loads to climate—evaluating state level sensitivities and vulnerabilities. *Energy* **2001**, *26*, 645–657.

(9) Franco, G.; Sanstad, A. Climate change and electricity demand in California. *Climatic Change* **2008**.

(10) Tennessee Valley Authority. Improving Load Factor and Power Factor to Reduce Demand. *Electrical Energy Managment Guidelines Series*. 2006, pp. 1–4.

(11) Sadugol, S. S. R. Effect of System Load Factor on Transmission & Distribution Losses. *IOSR Journal of Electrical and Electronics Engineering* **2012**, *2*, 1–6.

(12) NYISO. *Power Trends 2012: State of the Grid*; 2012.

(13) Harris Williams & Co. *ESCOs – Enabling Energy Efficiency White Paper*; 2010.

(14) State Energy Planning Board. *Electricity Assessment: Resources and Markets New York State Energy Plan 2009*; 2009.

(15) White, C. D.; Zhang, K. M. Using vehicle-to-grid technology for frequency regulation and peak-load reduction. *Journal of Power Sources* **2011**, *196*, 3972–3980.

(16) Proctor Engineering Group. *HVAC Pacific Gas & Electric Company White Paper*; 2004; pp. 1–13.

(17) Arteconi, A.; Hewitt, N. N. J.; Polonara, F. State of the art of thermal storage for demand-side management. *Applied Energy* **2012**, *93*, 371–389.

(18) Dincer, I. On thermal energy storage systems and applications in buildings. *Energy and Buildings* **2002**, *34*, 377–388.

(19) Henze, G. P. An Overview of Optimal Control for Central Cooling Plants with Ice Thermal Energy Storage. *Journal of Solar Energy Engineering* **2003**, *125*, 302.

(20) Braun, J. E. Braun A comparison of chiller-priority, storage-priority, and optimial control of an ice-storage system. *ASHRAE Transactions* **1992**, *98 1*, 893–902.

(21) Henze, G. P.; Krarti, M.; Brandemuehl, M. J. Guidelines for improved performance of ice storage systems. *Energy and Buildings* **2003**, *35*, 111–127.

(22) Henze, G.; Dodier, R.; Krarti, M. Development of a Predictive Optimal Controller for Thermal Energy Storage Systems. *HVAC&R Research* **1997**, *3*, 233–264.

(23) Al-Qalamchi, A. A.; Adil, A. Performance of ice storage system utilizing a combined partial and full storage strategy. *Desalination* **2007**, *209*, 306–311.

(24) Hajiah, A.; Krarti, M. Optimal controls of building storage systems using both ice storage and thermal mass – Part II: Parametric analysis. *Energy Conversion and Management* **2012**, *64*, 509–515.

(25) Wang, J.-J.; Zhang, C.-F.; Jing, Y.-Y.; Zheng, G.-Z.; Jiang-jiang, W.; Chun-fa, Z.; You-yin, J.; Guo-zhong, Z. Using the fuzzy multi-criteria model to select the optimal cool storage system for air conditioning. *Energy and Buildings* **2008**, *40*, 2059–2066.

(26) Lee, W.; Chen, Y.; Wu, T. Optimization for ice-storage air-conditioning system using particle swarm algorithm. *Applied Energy* **2009**, *86*, 1589–1595.

(27) Sehar, F.; Rahman, S.; Pipattanasomporn, M. Impacts of ice storage on electrical energy consumptions in office buildings. *Energy and Buildings* **2012**, *51*, 255–262.

(28) Henze, G. P. Impact of real-time pricing rate uncertainty on the annual performance of cool storage systems. *Energy and Buildings* **2003**, *35*, 313–325.

(29) Chen, H.-J.; Wang, D. W. P.; Chen, S.-L. Optimization of an ice-storage air conditioning system using dynamic programming method. *Applied Thermal Engineering* **2005**, *25*, 461–472.

(30) U.S. Energy Information Administration. Annual Energy Review:Electricity http://www.eia.gov/totalenergy/data/annual/index.cfm (accessed Jul 1, 2013).

(31) LaCommare, K. H.; Eto, J. H. *Understanding the Cost of Power Interruptions to U.S. Electricity Consumers*; 2004.

(32) Lefton, S.; Kumar, N.; Hilleman, D.; Agan, D. A New Paradigm: Cycling Operations at Nuclear Power Plants in the United States. In *ASME Power Conference*; 2013.

(33) Lefton, S.; Hilleman, D. Make Your Plant Ready for Cycling Operations. *POWER*. August 2011,.

(34) U.S. Energy Information Administration. Summary Statistics for the United States http://www.eia.gov/electricity/ (accessed Oct 10, 2010).

(35) Valentine, K.; Temple, W. G.; Zhang, K. M. Intelligent electric vehicle charging: Rethinking the valley-fill. *Journal of Power Sources* **2011**, *196*, 10717–10726.

(36) NYSERDA. *Patterns and Trends New York State Energy Profiles : 1997-2011*; 2013; pp. 1997–2011.

(37) U.S. Energy Information Administration. U.S. Census Regions and Divisions Map for Commercial Buildings http://www.eia.gov/consumption/commercial/census-maps.cfm (accessed Oct 18, 2010).

(38) United States Census Bureau. New York Quick Fact http://quickfacts.census.gov/qfd/states/36000.html (accessed Oct 20, 2010).

(39) U.S. Energy Information Administration. 2003 CBECS Detailed Tables: Summary http://www.eia.gov/consumption/commercial/ (accessed Oct 10, 2010).

(40) Stocki, M.; Curcija, D. C.; Bhandari, M. S. The Development of Standardized Whole-Building Simulation Assumptions for Energy Analysis. *ASHRAE Transactions* **2007**, *113*, 422–436.

(41) U.S. Energy Information Administration. 2006 Manufacturing Energy Data Tables http://www.eia.gov/consumption/manufacturing/ (accessed Oct 17, 2010).

(42) Bekker, B.; Carew, P. *Reducing energy consumption by designing for chiller efficiency*; 2010.

(43) University of Wisconsin. TRNSYS User Manual, 2012.

(44) Valentine, K. F.; Temple, W. G.; Zhang, K. M. Electric vehicle charging and wind power integration: Coupled or decoupled electricity market resources? *2012 IEEE Power and Energy Society General Meeting* **2012**, 1–7.

(45) Tanaka, M. Real-time pricing with ramping costs: A new approach to managing a steep change in electricity demand. *Energy Policy* **2006**, *34*, 3634–3643.

(46) NYISO. Open Access Transmission & Market Administration and Control Area Services Tariffs: Schedule 1 Rates for July 2006., 2006.

(47) Jeon, W.; Mo, J. Y.; Mount, T. D. Developing a Smart Grid that Customers can Afford : The Impact of Deferrable Demand. *Energy* **2014**.

(48) NYISO. ICAP Data & Information http://www.nyiso.com/public/markets_operations/market_data/icap/index.jsp (accessed Jul 29, 2014).

(49) Westcott, A. ICAP/UCAP Overview, 2012.

(50) Borenstein, S. *The Trouble With Electricity Markets (and some solutions)*; POWER; 081; 2001.

(51) Wight, D.; Daly, C.; Kathan, D.; Lee, M.; Martin, K.; Silberstein, P.; Tita, M.; Vertes, R. *Assessment of Demand Response and Advanced Metering*; 2010.

(52) Henze, G. P. Energy and Cost Minimal Control of Active and Passive Building Thermal Storage Inventory. *Journal of Solar Energy Engineering* **2005**, *127*, 343.

(53) Akbari, H. Performance evaluation of thermal energy storage systems. *Energy and Buildings* **1995**, *22*, 15–24.

(54) Ma, Y.; Borrelli, F.; Hencey, B. Model predictive control of thermal energy storage in building cooling systems. *Decision and Control, …* **2009**, 392–397.

(55) Newell, S.; Faruqui, A. Dynamic Pricing: Potential Wholesale Market Benefits in New York State, 2009, *12144*.

(56) Faruqui, A.; Hledik, R.; Tsoukalis, J. The power of dynamic pricing. *The Electricity Journal* **2009**.

(57) Hansen, D. G.; Armstrong, D. A. *The Effects of Critical Peak Pricing for Commercial and Industrial Customers for the Kansas Corporation Commission Final Report*; 2012.

(58) Boisvert, R.; Cappers, P.; Neenan, B. The benefits of customer participation in wholesale electricity markets. *The Electricity Journal* **2002**, *6190*, 41–51.

(59) U.S. Department of Energy. Commercial Prototype Building Models www.energycodes.gov/development/commercial/90.1_models (accessed Aug 10, 2012).

(60) TESS. TRNSYS, 2008.

(61) Weather Underground www.wunderground.com/ (accessed Jul 25, 2012).

(62) U.S. EPA. National Action Plan for Energy Efficiency Sector Collaborative on Energy Efficiency Office Building Energy Use Profile. **2003**, 1–4.

(63) U.S. Department of Energy. Energy Efficiency Trends in Residential and Commercial Buildings. **2008**.

(64) Westphalen, D.; Koszalinski, S. *Energy Consumption Characteristics of Commercial Building HVAC Systems*; 1999; Vol. II.

(65) U.S. Department of Energy. Buildings Energy Data Book: Commercial Sector http://buildingsdatabook.eren.doe.gov/ChapterIntro3.aspx (accessed Oct 15, 2012).

(66) TRANE. Air-Cooled Liquid Chillers. *TRANE*, 2004.

(67) North Carolina Energy Office. Chillers: Energy saving fact sheet. *North Carolina Energy Office*, 2010.

(68) Hornberger, M. ICEPIT: Simulationsprogramm für vertikal geschichteten Erdbecken-Speicher zur Wärme- und Kältespeicherung, 2006.

(69) Christophe, A.; Philippe, A. ICE STORAGE SYSTEM (ISS): SIMULATION OF A TYPICAL HVAC PRIMARY PLANT EQUIPPED WITH AN ICE STORAGE UNIT. *IBPSA* **2003**, 47–54.

(70) Henze, G. P. Parametric Study of a Simplified Ice Storage Model Operating Under Conventional and Optimal Control Strategies. *Journal of Solar Energy Engineering* **2003**, *125*, 2.

(71) ConEdison of New York. PSC NO:10- Electricity, 2012.

(72) ConEdison. Demand Response Program Comparison Guide - Business Customers http://www.naruc.org/international/Documents/Demand Response Comparison Chart1.pdf (accessed Feb 5, 2014).

(73) Akter, M. NYISO 2012 Annual Report on Demand Response Programs, 2013, *4*.

(74) NYISO. NYISO Tariffs: Emergency Demand Response Program, 2011.

(75) Atabay, D.; Herzog, S.; Sanger, F.; Jungwirth, J.; Mikulovic, V. Self-Adapting Building Models and Optimized HVAC Scheduling for Demand Side Management. *22nd International Conference on Electricity Distribution* **2013**.

(76) Wetter, M.; Wright, J. Comparison of a Generalized Pattern Search and Genetic Algorithm Optimization Method. In *Eight International IBPSA Conference*; Eindhoven, Netherlands, 2003; pp. 1401–1408.

(77) Caramia, M.; Dell'Olmo, P. Multi-objective Optimization. In *Multi-objective Managment in Freight Logistics: Increasing Capacity, Service Level and Safety with Optimization Algorithms*; Springer; pp. 11–376.

(78) Kirby, B. *Spinning Reserve From Responsive Loads*; 2003.

(79) Eto, J. H.; Nelson-Hoffman, J.; Torres, C.; Hirth, S.; Yinger, B.; Kueck, J.; Kirby, B.; Bernier, C.; Wright, R.; Barat, A.; et al. ERNEST ORLANDO LAWRENCE Demand Response Spinning Reserve Demonstration. **2007**.

(80) Walawalkar, R.; Apt, J.; Mancini, R. Economics of electric energy storage for energy arbitrage and regulation in New York. *Energy Policy* **2007**, *35*, 2558–2568.

(81) Patton, D. B.; VanSchaick, P. L.; Chen, J. *2012 State of the Market Report for the New York ISO Markets*; 2013.

(82) Ellison, J.; Tesfatsion, L. *Project Report: A Survey of Operating Reserve Markets in US ISO/RTO-managed Electric Energy Regions*; 2012.

(83) Patton, D. B.; Leevanschaick, P.; Chen, J. *2010 State of the Market Report for the New York ISO Markets*; 2011.

(84) Wood, A.; Woolenberg, B.; Sheble, G. *Power Generation, Operation and Control*; 2nd ed.; Wiley, 1996.

(85) NYISO. NYISO Spinning Reserve Deployment http://www.nyiso.com/public/markets_operations/market_data/reports_info/index.jsp (accessed May 28, 2014).

(86) NYISO. NYC Load Data http://www.nyiso.com/public/markets_operations/market_data/load_data/index.jsp (accessed May 1, 2014).

(87) NYISO. NYISO Markets & Operations: Pricing Data http://www.nyiso.com/public/markets_operations/market_data/pricing_data/index.jsp (accessed Feb 1, 2013).

(88) AWEA. *U.S. Wind Industry Annual Market Report 2013*; 2014.

(89) Rocky Mountain Institute. 2050 generation by Case http://www.rmi.org/RFGraph-2050_generation_by_case (accessed Apr 25, 2014).

(90) Holttinen, H.; Meibom, P.; Orths, A.; Hulle, F. Van; Lange, B. *IEA Wind Task 25 Design and operation of power systems with large amounts of*; 2006.

(91) Saintcross, J. *The effects of integrating wind power on transmission system planning, reliability, and operations*; 2005.

(92) Corbus, D.; King, J.; Mousseau, T. *Eastern wind integration and transmission study*; 2010.

(93) Ela, E.; Milligan, M.; Parsons, B.; Lew, D.; Corbus, D. The evolution of wind power integration studies: Past, present, and future. *2009 IEEE Power & Energy Society General Meeting* **2009**, 1–8.

(94) Smith, J.; Milligan, M. Utility wind integration and operating impact state of the art. *IEEE Transactions on Power Systems* **2007**, *22*, 900–908.

(95) Ackermann, T.; Kuwahata, R. Lessons learned from international wind integration studies. *Energynautics GmbH. Langen, Germany* **2011**, *4*.

(96) Milligan, M.; Donohoo, P.; Lew, D.; Ela, E. *Operating reserves and wind power integration: an international comparison*; 2010.

(97) EnerNex Corporation. *Avista Corporation Wind Integration Study*; 2007.

(98) Acker, T.; Buechler, J.; Broome, S.; Potter, C. Arizona Public Service Wind Integration Cost Impact Study. **2007**.

(99) Lew, D.; Brinkman, G.; Ibanez, E.; Florita, A.; Heaney, M.; Hodge, B.; Hummon, M.; King, J. The Western Wind and Solar Integration Study Phase 2 The Western Wind and Solar Integration Study Phase 2. **2013**.

(100) Ela, E.; Navid, N. MISO and NREL Collaboration - Operating Reserves Research, 2011.

(101) NESCAUM. *Air Quality, Electricity, and Back-up Stationary Diesel Engines in the Northeast*; 2012.

(102) Frontier Economics. Impacts of climate change policies on generation investment and operation. **2008**.